

# Probabilistic Verification of Neural Networks using Branch and Bound

David Boetius <sup>1</sup>, Stefan Leue <sup>1</sup>, and Tobias Sutter <sup>1</sup>

<sup>1</sup>University of Konstanz  
{[david.boetius](mailto:david.boetius@uni-konstanz.de), [stefan.leue](mailto:stefan.leue@uni-konstanz.de), [tobias.sutter](mailto:tobias.sutter@uni-konstanz.de)}@uni-konstanz.de

29th May 2024

## Abstract

Probabilistic verification of neural networks is concerned with formally analysing the output distribution of a neural network under a probability distribution of the inputs. Examples of probabilistic verification include verifying the demographic parity fairness notion or quantifying the safety of a neural network. We present a new algorithm for the probabilistic verification of neural networks based on an algorithm for computing and iteratively refining lower and upper bounds on probabilities over the outputs of a neural network. By applying state-of-the-art bound propagation and branch and bound techniques from non-probabilistic neural network verification, our algorithm significantly outpaces existing probabilistic verification algorithms, reducing solving times for various benchmarks from the literature from tens of minutes to tens of seconds. Furthermore, our algorithm compares favourably even to dedicated algorithms for restricted subsets of probabilistic verification. We complement our empirical evaluation with a theoretical analysis, proving that our algorithm is sound and, under mildly restrictive conditions, also complete when using a suitable set of heuristics.

## 1 Introduction

As deep learning spreads through society, it becomes increasingly important to ensure the reliability of artificial neural networks, including aspects of fairness and safety. However, manually introspecting neural networks is infeasible due to their opaque nature, and empirical assessments of neural networks are challenged by neural networks being fragile with respect to various types of input perturbations [11, 17, 23, 29, 30, 32, 53]. In contrast, neural network verification analyses neural networks with mathematical rigour, facilitating the faithful auditing of neural networks.

In this paper, we consider probabilistic verification of neural networks, which is concerned with proving statements about the output distribution of a neural network. An example of probabilistic verification is proving that a neural network net making a binary decision affecting a person (for example, hire/do not hire, credit approved/denied) satisfies the demographic parity fairness notion [7] under a probability distribution  $\mathbb{P}_{\mathbf{x}}$  of the network inputs  $\mathbf{x}$  representing the person

$$\frac{\mathbb{P}_{\mathbf{x}}[\text{net}(\mathbf{x}) = \text{yes} \mid \mathbf{x} \text{ is disadvantaged}]}{\mathbb{P}_{\mathbf{x}}[\text{net}(\mathbf{x}) = \text{yes} \mid \mathbf{x} \text{ is advantaged}]} \geq \gamma, \quad (1)$$

where  $\gamma \in [0, 1]$  with  $\gamma = 0.8$  being a common choice [25]. A closely related problem to probabilistic verification is computing bounds on probabilities over a neural network. An example of this is quantifying the safety of a neural network by bounding

$$\mathbb{P}_{\mathbf{x}}[\text{net}(\mathbf{x}) \text{ is unsafe}]. \quad (2)$$

In this paper, we introduce a novel algorithm for computing bounds on probabilities such as Equation (2) using a branch and bound framework [37, 44]. These bounds then allow us to verify probabilistic statements like Equation (1) using ideas from the probabilistic verification algorithm FairSquare [3].

More concretely, we recombine neural network verification using branch and bound [15], linear relaxations of neural networks [52, 67], and massively parallel branch and bound [65] with ideas from FairSquare [3] for probabilistic neural network verification, to obtain the Probabilistic Verification (PV) algorithm, a fast and generally applicable probabilistic verification algorithm for neural networks. Our theoretical analysis of PV shows that PV is sound and, under mildly restrictive conditions, complete when using suitable branching and splitting heuristics.

Our experimental evaluation reveals that PV significantly outpaces the probabilistic verification algorithms FairSquare [3] and SpaceScanner [19]. In particular, we solve benchmark instances that FairSquare can not solve within 15 minutes in less than 10 seconds and solve the ACAS Xu [34] probabilistic robustness case study of Converse et al. [19] in a mean runtime of 18 seconds, compared to 33 minutes for SpaceScanner.

Applying PV to #DNN verification [38], a subset of probabilistic verification, reveals that PV also compares favourably to the ProVe\_SLR algorithm [40] specialised to #DNN verification and even the  $\varepsilon$ -ProVe algorithm [39] that relaxes #DNN verification to computing a confidence interval on the solution. In contrast to  $\varepsilon$ -ProVe and similar approaches [6, 8, 60], PV computes lower and upper bounds on probabilities like Equation (2) that are guaranteed to hold with absolute certainty. Such bounds are preferable to confidence intervals in high-risk machine-learning applications.

To test the limits of PV and fuel further research in probabilistic verification, we introduce a significantly more challenging probabilistic verification benchmark: MiniACSIncome is a benchmark based on the ACSIncome dataset [20] and is concerned with verifying the demographic parity of neural networks for datasets of increasing input dimensionality. In summary, our contributions are

- the PV algorithm for the probabilistic verification of neural networks,
- a theoretical analysis of PV,
- a thorough experimental comparison of PV with existing probabilistic verifiers for neural networks and tools dedicated to restricted subsets of probabilistic verification, and
- MiniACSIncome: a new, challenging probabilistic verification benchmark.

## 2 Related Work

Non-probabilistic neural network verification is concerned with proving that the outputs of a neural network satisfy some condition for all inputs in an input set. Approaches for non-probabilistic neural network verification include Satisfiability Modulo Theories (SMT) solving [21, 34, 63], Mixed Integer Linear Programming (MILP) [4, 18, 54], and Reachability Analysis [5, 55, 56]. Many of these approaches can be understood as branch and bound algorithms [15]. Branch and bound [37, 44] also powers the  $\alpha, \beta$ -CROWN [66], MN-BaB [26] and VeriNet [31] verifiers that lead the table in recent international neural network verifier competitions [14, 45].

A critical component of a branch and bound verification algorithm is computing bounds on the output of a neural network. Approaches for bounding neural network outputs include interval arithmetic [18, 50], dual approaches [62], linear bound propagation techniques [52, 61, 67], multi-neuron linear relaxations [46], and further optimisation-based approaches [16, 47, 65].

Probabilistic verification algorithms can be divided into *sound* algorithms that provide valid proofs and *probably sound* algorithms that provide valid proofs with a certain predefined probability. FairSquare [3] is a fairness verification algorithm, a subset of probabilistic verification that studies

problems such as Equation (1). FairSquare uses SMT solving for splitting the input space into disjoint hyperrectangles, integrating over which yields bounds on a target probability. Converse et al. [19] (SpaceScanner) and Borca-Tasciuc et al. [13] divide the input space into disjoint polytopes using concolic execution and reachable set verification, respectively, to perform probabilistic verification. Morettin et al. [43] use weighted model integration [10] to obtain a general probabilistic verification algorithm but neither provide code nor report runtimes. A restricted subset of probabilistic verification is #DNN verification [38], corresponding to probabilistic verification under uniformly distributed inputs. The #DNN verifier ProVe\_SLR [40] uses a similar massively parallel branch and bound approach as our algorithm but does not perform general probabilistic verification.

Probably sound verification algorithms [6, 8, 38, 39] obtain efficiency at the cost of potentially unsound results.  $\epsilon$ -ProVe [39] is a probably sound #DNN verification algorithm. Bastani et al. [8], Converse et al. [19] and Marzari et al. [40] compare sound and probably sound approaches for fairness verification, general probabilistic verification, and #DNN verification, respectively. We study sound probabilistic verification since certainly sound results are preferable in critical applications, such as education [24], medical applications, or autonomous driving and flight.

Besides probabilistic fairness notions, such as demographic parity [7], several approaches [12, 41, 51, 57] verify *dependency fairness* [27, 57], an individual fairness notion [22] that states that persons that only differ by their protected attribute (for example, gender or race) need to be assigned to the same class. However, dependency fairness can be satisfied trivially by withholding the protected attribute from the classifier. Since withholding the protected attribute is insufficient [49] or even harmful [36] for fairness, dependency fairness is an insufficient fairness notion.

### 3 Preliminaries and Problem Statement

Throughout this paper, we are concerned with computing (provable) lower and upper bounds on various functions.

**Definition 1** (Bounds). For  $f : \mathbb{R}^n \rightarrow \mathbb{R}^m$ , we call  $\ell, u \in \mathbb{R}^m$  a *lower*, respectively, *upper bound* on  $f$  for  $\mathcal{X}' \subseteq \mathbb{R}^n$  if  $\ell \leq f(\mathbf{x}) \leq u, \forall \mathbf{x} \in \mathcal{X}'$ .

**Neural Networks.** In particular, we are concerned with computing bounds on functions involving neural networks  $\text{net} : \mathcal{X} \rightarrow \mathbb{R}^m$ , where  $\mathcal{X} \subset \mathbb{R}^n$  is the input space of the neural network. A neural network is a composition of linear functions and a predefined set of non-linear functions, such as ReLU, Tanh, and max pooling. We refrain from further defining neural networks but refer the interested reader to the auto\_LiRPA library [64] that practically defines the class of neural networks to which our algorithm can be applied. For the scope of this paper, we only consider fully-connected feed-forward neural networks.

Throughout this paper, we assume that the input space  $\mathcal{X}$  is a bounded hyperrectangle. Bounded input spaces are common in machine learning. Examples include the space of normalised images  $[0, 1]^n$  in computer vision and tabular input spaces of practically bounded variables, such as age, working hours per week, income, etc.

**Notation and Terminology.** We use bold letters ( $\mathbf{x}, \mathbf{y}$ ) for vectors and calligraphic letters ( $\mathcal{X}$ ) for sets. Let  $\underline{\mathbf{x}}, \bar{\mathbf{x}} \in \mathbb{R}^n$  with  $\underline{\mathbf{x}} \leq \bar{\mathbf{x}}$ . We use  $[\underline{\mathbf{x}}, \bar{\mathbf{x}}] = \{\mathbf{x} \in \mathbb{R}^n \mid \underline{\mathbf{x}} \leq \mathbf{x} \leq \bar{\mathbf{x}}\}$  to denote the hyperrectangle with the minimal element  $\underline{\mathbf{x}}$  and the maximal element  $\bar{\mathbf{x}}$ . When we speak of *bounds* on a certain quantity in this paper, we refer to a pair of a lower and an upper bound. Throughout this paper,  $\ell, k$  denote lower bounds, and  $u$  denotes an upper bound. When convenient, we also use  $\underline{\mathbf{y}} \leq \mathbf{y} \leq \bar{\mathbf{y}}$  to denote bounds, especially on vectors. We assume that all random objects are defined on the same abstract probability space  $(\Omega, \mathcal{F}, \mathbb{P})$  and that all continuous random variables admit a probability density function.

### 3.1 Probabilistic Verification of Neural Networks

Let  $\mathcal{X} \subset \mathbb{R}^n$  be a bounded hyperrectangle and let  $v \in \mathbb{N}$ . In this paper, we are concerned with proving or disproving whether  $\text{net} : \mathcal{X} \rightarrow \mathbb{R}^m$  is feasible for the *probabilistic verification problem*

$$P : \begin{cases} f_{\text{Sat}}(p_1, \dots, p_v) \geq 0, \\ p_i = \mathbb{P}_{\mathbf{x}^{(i)}}[g_{\text{Sat}}^{(i)}(\mathbf{x}^{(i)}, \text{net}(\mathbf{x}^{(i)})) \geq 0] \quad \forall i \in \{1, \dots, v\}, \end{cases} \quad (3)$$

where  $\mathbf{x}^{(i)}, i \in \{1, \dots, v\}$ , is a  $\mathcal{X}$ -valued random variable with distribution  $\mathbb{P}_{\mathbf{x}^{(i)}}$  and  $f_{\text{Sat}} : \mathbb{R}^v \rightarrow \mathbb{R}, g_{\text{Sat}}^{(i)} : \mathbb{R}^n \times \mathbb{R}^m \rightarrow \mathbb{R}, i \in \{1, \dots, v\}$  are *satisfaction functions*. We only consider satisfaction functions that are compositions of linear functions, multiplication, division, and monotone functions, such as ReLU, Sigmoid, min and max. Throughout this paper, we assume all probabilistic verification problems to be well-defined.

**Example 1.** We express the demographic parity fairness notion from Equation (1) as a probabilistic verification problem. Let  $\mathcal{X} \subset \mathbb{R}^n$  be an input space containing a categorical protected attribute, such as gender, race, or disability status that is one-hot encoded at the indices  $A \subset \{1, \dots, n\}$ . We assume a single historically advantaged category encoded at the index  $a \in A$ . Consider a neural network  $\text{net} : \mathbb{R}^n \rightarrow \mathbb{R}^2$  that acts as a binary classifier making a decision affecting a person, such as hiring or credit approval. The neural network produces a score for each class and assigns the class with the higher score to an input. We express Equation (1) as a probabilistic verification problem, that is,

$$\frac{\mathbb{P}_{\mathbf{x}}[\text{net}(\mathbf{x}) = \text{yes} \mid \mathbf{x} \text{ is disadvantaged}]}{\mathbb{P}_{\mathbf{x}}[\text{net}(\mathbf{x}) = \text{yes} \mid \mathbf{x} \text{ is advantaged}]} \geq \gamma \iff \text{net is feasible in Equation (3),}$$

where,  $f_{\text{Sat}}(p_1, p_2, p_3, p_4) = (p_1 p_4)/(p_2 p_3) - \gamma, g_{\text{Sat}}^{(1)}(\mathbf{x}, \text{net}(\mathbf{x})) = \min(\text{net}(\mathbf{x})_1 - \text{net}(\mathbf{x})_2, -\mathbf{x}_a), g_{\text{Sat}}^{(2)}(\mathbf{x}, \text{net}(\mathbf{x})) = -\mathbf{x}_a, g_{\text{Sat}}^{(3)}(\mathbf{x}, \text{net}(\mathbf{x})) = \min(\text{net}(\mathbf{x})_1 - \text{net}(\mathbf{x})_2, \mathbf{x}_a - 1),$  and  $g_{\text{Sat}}^{(4)}(\mathbf{x}, \text{net}(\mathbf{x})) = \mathbf{x}_a - 1$ . Appendix A contains a detailed derivation of this equivalence.

If all inputs  $\mathbf{x}^{(i)}$  are uniformly distributed, probabilistic verification corresponds to #DNN verification [38]. As Marzari et al. [38] prove, #DNN verification is #P complete, implying that probabilistic verification is #P hard. Since #P is at least as hard as NP, we can not expect to obtain efficient algorithms, but which probabilistic verification problems are practically solvable remains undetermined.

### 3.2 Non-Probabilistic Neural Network Verification

The goal of non-probabilistic neural network verification is to prove or disprove whether a neural network  $\text{net} : \mathcal{X} \rightarrow \mathbb{R}^m$  is feasible for

$$V : g_{\text{Sat}}(\mathbf{x}, \text{net}(\mathbf{x})) \geq 0 \quad \forall \mathbf{x} \in \mathcal{X}', \quad (4)$$

where  $\mathcal{X}' \subseteq \mathcal{X}$  is a hyperrectangle, and  $g_{\text{Sat}} : \mathbb{R}^n \times \mathbb{R}^m \rightarrow \mathbb{R}$  is a *satisfaction function* that indicates whether the output of  $\text{net}$  is desirable ( $g_{\text{Sat}}(\cdot, \text{net}(\cdot)) \geq 0$ ) or undesirable ( $g_{\text{Sat}}(\cdot, \text{net}(\cdot)) < 0$ ). In (non-probabilistic) neural network verification,  $g_{\text{Sat}}$  can generally be considered a part of  $\text{net}$  [15, 64]. *Neural network verifiers* are algorithms for proving or disproving Equation (4). Two desirable properties of neural network verifiers are *soundness* and *completeness*.

**Definition 2** (Soundness and Completeness). A verification algorithm is *sound* if it only produces genuine counterexamples and valid proofs for Equation (4). It is *complete* if it produces a counterexample or proof for Equation (4) for any neural network in a finite amount of time.

Analogous notions of soundness and completeness also apply to probabilistic verifiers. Generally unsound but *probably sound* probabilistic verification approaches are discussed in Section 2. We introduce incomplete and complete neural network verification through two examples: interval arithmetic and branch and bound.

### 3.2.1 Interval Arithmetic

Interval arithmetic [42] is a bound propagation technique that derives bounds on the output of a neural network from bounds on the network input. Assume  $\underline{\mathbf{x}} \leq \mathbf{x} \leq \bar{\mathbf{x}}$  are bounds on the network input  $\mathbf{x}$  and we apply interval arithmetic to compute  $\ell \leq g_{\text{Sat}}(\mathbf{x}, \text{net}(\mathbf{x})) \leq u, \forall \mathbf{x} \in [\underline{\mathbf{x}}, \bar{\mathbf{x}}]$ . If the lower bound is large enough or the upper bound small enough, we can prove or disprove Equation (4) using

$$\ell \geq 0 \implies g_{\text{Sat}}(\mathbf{x}, \text{net}(\mathbf{x})) \geq 0, \quad \text{respectively,} \quad u < 0 \implies g_{\text{Sat}}(\mathbf{x}, \text{net}(\mathbf{x})) < 0.$$

However, if the bounds are *inconclusive*, that is  $\ell < 0 \leq u$ , we can neither prove nor disprove Equation (4). The possibility of inconclusive results makes interval arithmetic an incomplete technique for neural network verification. In particular, interval arithmetic is relatively imprecise, meaning that bounds derived using interval arithmetic are frequently inconclusive [28]. More precise approaches include DeepPoly [52] and CROWN [67] that follow the same overall scheme but propagate *linear bounds* through a neural network. We primarily employ interval arithmetic to compute bounds on the  $f_{\text{Sat}}$  function in Equation (3) given bounds on  $p_1, \dots, p_v$ .

Let  $f : \mathbb{R}^n \rightarrow \mathbb{R}$  be a function that we want to bound for inputs  $\mathbf{x} \in [\underline{\mathbf{x}}, \bar{\mathbf{x}}]$ . Interval arithmetic and other bound propagation techniques rely on  $f = f^{(K)} \circ \dots \circ f^{(1)}$  being a composition of more fundamental functions  $f^{(k)} : \mathbb{R}^{n_k} \rightarrow \mathbb{R}^{n_{k+1}}$  for which we can already compute  $\ell^{(k)} \leq f^{(k)}(\mathbf{z}) \leq u^{(k)}$  given  $\underline{\mathbf{z}} \leq \mathbf{z} \leq \bar{\mathbf{z}}$ . Examples of such functions include monotone non-decreasing functions, for which  $f^{(k)}(\underline{\mathbf{z}}) \leq f^{(k)}(\mathbf{z}) \leq f^{(k)}(\bar{\mathbf{z}})$ , or monotone non-increasing functions, for which  $f^{(k)}(\bar{\mathbf{z}}) \leq f^{(k)}(\mathbf{z}) \leq f^{(k)}(\underline{\mathbf{z}})$ . These two *bounding rules* already allow us to bound addition, subtraction, min, max, and many popular neural network activation functions like ReLU, Sigmoid, and Tanh. Appendix B contains bounding rules for linear functions, multiplication, and division. Algorithm 1 describes how interval arithmetic computes bounds on  $f$  using the bounding rules for  $f^{(K)} \dots, f^{(1)}$ .

---

#### Algorithm 1: Interval Arithmetic

---

**Input:** Function  $f = f^{(K)} \circ \dots \circ f^{(1)}$ , Input Bounds  $\underline{\mathbf{x}}, \bar{\mathbf{x}}$

- 1  $\underline{\mathbf{z}}^{(0)} \leftarrow \underline{\mathbf{x}}, \bar{\mathbf{z}}^{(0)} \leftarrow \bar{\mathbf{x}}$
- 2 **for**  $k \in \{1, \dots, K\}$  **do**  $(\underline{\mathbf{z}}^{(k)}, \bar{\mathbf{z}}^{(k)}) \leftarrow \text{BoundingRule}(f^{(k)}, \underline{\mathbf{z}}^{(k-1)}, \bar{\mathbf{z}}^{(k-1)})$
- 3 **return**  $\underline{\mathbf{z}}^{(K)}, \bar{\mathbf{z}}^{(K)}$

---

### 3.2.2 Branch and Bound

Irrespective of their relative precision, bound propagation approaches such as interval arithmetic, DeepPoly [52], and CROWN [67] are incomplete according to Definition 2. To obtain a complete verifier, bound propagation can be combined with *branching* to gain completeness. This algorithmic framework is called *branch and bound* [15, 37, 44]. In branch and bound, when the computed bounds are inconclusive ( $\ell < 0 \leq u$ ), the search space is split (*branching*). The idea is that splitting improves the precision of the bounds for each part of the split (each *branch*).

Algorithm 2 contains an abstract branch and bound algorithm for neural network verification. This algorithm has three subprocedures that we need to instantiate for running Algorithm 2: Select, ComputeBounds, and Split. One instantiation that yields a complete algorithm is selecting branches in a FIFO order, computing bounds using interval arithmetic and splitting the search space by bisecting the input space [59]. Xu et al. [65] present an improved complete branch and bound algorithm that selects branches in batches to utilise massively parallel hardware such as GPUs, computes bounds using a combined bound propagation and optimisation procedure, and splits the search space by splitting on hidden ReLU nodes in the network [58]. We refer to Zhang et al.



[66] for a state-of-the-art neural network verifier [14, 45] based on branch and bound. In the next section, we introduce a branch and bound algorithm for the probabilistic verification of neural networks.

---

**Algorithm 2:** Branch and Bound for Non-Probabilistic Neural Network Verification

---

**Input:** Verification Problem  $g_{\text{Sat}}(\mathbf{x}, \text{net}(\mathbf{x})) \geq 0, \forall \mathbf{x} \in \mathcal{X}'$  where  $\mathcal{X}' = [\underline{\mathbf{x}}, \bar{\mathbf{x}}]$

- 1 branches  $\leftarrow \{\mathcal{X}'\}$
- 2 **while** branches  $\neq \emptyset$  **do**
- 3      $[\underline{\mathbf{x}}', \bar{\mathbf{x}}'] \leftarrow \text{Select}(\text{branches})$  (Select one branch)
- 4      $(\underline{y}, \bar{y}) \leftarrow \text{ComputeBounds}(g_{\text{Sat}}(\cdot, \text{net}(\cdot)), \underline{\mathbf{x}}, \bar{\mathbf{x}})$  (E.g. interval arithmetic)
- 5     **if**  $\bar{y} < 0$  **then return** Violated (Every  $\mathbf{x} \in [\underline{\mathbf{x}}', \bar{\mathbf{x}}']$  is a counterexample)
- 6     **else if**  $\underline{y} \geq 0$  **then** branches  $\leftarrow (\text{branches} \setminus \{[\underline{\mathbf{x}}', \bar{\mathbf{x}}']\})$  (Prune branch)
- 7     **else**
- 8         new  $\leftarrow \text{Split}([\underline{\mathbf{x}}', \bar{\mathbf{x}}'])$  (E.g. by bisection)
- 9         branches  $\leftarrow (\text{branches} \setminus \{[\underline{\mathbf{x}}', \bar{\mathbf{x}}']\}) \cup \text{new}$
- 10 **return** Satisfied (All branches pruned)

---

## 4 Algorithm

This section introduces Probabilistic Verification (PV), our algorithm for probabilistic verification of neural networks as defined in Equation (3). For conciseness, we use  $p_i$  for  $i \in \{1, \dots, v\}$  as in Equation (3) and drop the index and superscripts <sup>(i)</sup> whenever we only consider a single probability  $p$ . PV uses the same overall approach as FairSquare [3]: Iteratively refine bounds on each  $p_i$  until interval arithmetic allows us to prove or disprove  $f_{\text{Sat}}(p_1, \dots, p_v) \geq 0$  (see Section 3.2.1). We also follow FairSquare in splitting the input space into hyperrectangles since this allows for computing probabilities efficiently. However, while FairSquare uses expensive SMT solving for refining the input space, we use a branch and bound algorithm utilising computationally inexpensive input splitting and bound propagation techniques from non-probabilistic neural network verification for refining the input splitting. Figure 1 illustrates our approach for computing and refining bounds on a probability  $p$ . The following sections first introduce the algorithm that solves Equation (3) given bounds on  $p_1, \dots, p_v$  before introducing the algorithm for computing the bounds on each  $p_i$ .

### 4.1 Probabilistic Verification Algorithm

Algorithm 3 describes the PV algorithm. The centrepiece of PV is the procedure ProbabilityBounds for computing bounds  $\ell_i^{(t)} \leq p_i \leq u_i^{(t)}$  on a probability  $p_i$  from Equation (3). Given  $\ell_i^{(t)} \leq p_i \leq u_i^{(t)}$ , we apply interval arithmetic as introduced in Section 3.2.1 to prove or disprove  $f_{\text{Sat}}(p_1, \dots, p_v)$ . As described in Section 3.2.1, this analysis may be inconclusive. In this case, ProbabilityBounds refines  $\ell_i^{(t)}, u_i^{(t)}$  to obtain  $\ell_i^{(t+1)}, u_i^{(t+1)}$  with  $\ell_i^{(t)} \leq \ell_i^{(t+1)} \leq p_i \leq u_i^{(t+1)} \leq u_i^{(t)}$ . We again apply interval arithmetic to  $f_{\text{Sat}}(p_1, \dots, p_v)$ , this time using  $\ell_i^{(t+1)}, u_i^{(t+1)}$ . If the result remains inconclusive, we iterate refining the bounds on each  $p_i$  until we obtain a conclusive result. PV applies ProbabilityBounds for each  $p_i$  in parallel, making use of several CPU cores or several GPUs. Our main contribution is the ProbabilityBounds algorithm for computing a converging sequence of lower and upper bounds on  $p_i$ . Section 4.2 describes ProbabilityBounds in detail.

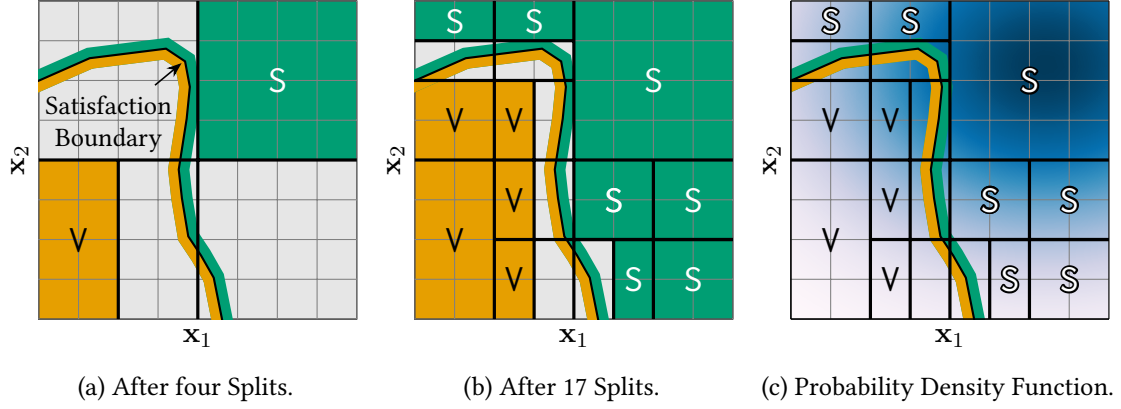

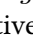


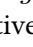


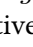



Figure 1: **Computing Bounds on Probabilities.** This figure illustrates the steps for computing bounds on  $p = \mathbb{P}_{\mathbf{x}}[g_{\text{Sat}}(\mathbf{x}, \text{net}(\mathbf{x})) \geq 0]$ . Our algorithm successively splits the input space to find regions that do not intersect the satisfaction boundary  $g_{\text{Sat}}(\mathbf{x}, \text{net}(\mathbf{x})) \geq 0$  (orange/green line ). Green, orange, and grey rectangles (, , ) denote regions for which we could prove  $g_{\text{Sat}}(\mathbf{x}, \text{net}(\mathbf{x})) \geq 0$  (satisfaction) ,  $g_{\text{Sat}}(\mathbf{x}, \text{net}(\mathbf{x})) < 0$  (violation) , or neither , respectively. By integrating the probability density  $f_{\mathbf{x}}$  in (c) (darker means higher density) over the green rectangles , we obtain a lower bound on  $p$ . Similarly, we can integrate over the orange rectangles  to construct an upper bound on  $p$ . Refining the input splitting from (a) to (b) tightens the bounds on  $p$ .

---

**Algorithm 3:** Probabilistic Verification (PV)

---

**Input:** Probabilistic Verification Problem as in Equation (3), Batch Size  $N$

```

1 for  $i \in \{1, \dots, v\}$  do           (Launch  $v$  parallel instances of ProbabilityBounds)
2    $PB_i \leftarrow \text{Launch ProbabilityBounds}(p_i, N)$ 
3 for  $t \in \mathbb{N}$  do
4   for  $i \in \{1, \dots, v\}$  do Gather  $\ell_i^{(t)}, u_i^{(t)}$  from  $PB_i$ 
5    $\ell^{(t)}, u^{(t)} \leftarrow \text{IntervalArithmetic}(f_{\text{Sat}}, (\ell_1^{(t)}, u_1^{(t)}), \dots, (\ell_v^{(t)}, u_v^{(t)}))$ 
6   if  $\ell^{(t)} \geq 0$  then return Satisfied
7   if  $u^{(t)} < 0$  then return Violated

```

---



---

**Algorithm 4:** ProbabilityBounds

---

**Input:** Probability  $\mathbb{P}_{\mathbf{x}}[g_{\text{Sat}}(\mathbf{x}, \text{net}(\mathbf{x})) \geq 0]$ , Batch Size  $N$

```

1 branches  $\leftarrow \{\mathcal{X}\}$            ( $\mathcal{X}$  is the input space of net)
2  $\ell^{(0)} \leftarrow 0, u^{(0)} \leftarrow 1$ 
3 for  $t \in \mathbb{N}$  do
4   batch  $\leftarrow \text{Select}(\text{branches}, N)$            (e.g., branches  $\mathcal{B}_i$  with largest  $\mathbb{P}_{\mathbf{x}}[\mathcal{B}_i]$ )
5    $(\underline{\mathbf{y}}, \bar{\mathbf{y}}) \leftarrow \text{ComputeBounds}(g_{\text{Sat}}(\cdot, \text{net}(\cdot)), \text{batch})$ 
6    $(\text{batch}, \mathcal{X}_{\text{sat}}^{(t)}, \mathcal{X}_{\text{viol}}^{(t)}) \leftarrow \text{Prune}(\text{batch}, \underline{\mathbf{y}}, \bar{\mathbf{y}})$ 
7    $\ell^{(t)} \leftarrow \ell^{(t-1)} + \mathbb{P}_{\mathbf{x}}[\mathcal{X}_{\text{sat}}^{(t)}]$ 
8    $u^{(t)} \leftarrow u^{(t-1)} - \mathbb{P}_{\mathbf{x}}[\mathcal{X}_{\text{viol}}^{(t)}]$ 
9   yield  $\ell^{(t)}, u^{(t)}$            (Report new bounds to PV)
10  new  $\leftarrow \text{Split}(\text{batch})$            (e.g., BaBSB [15])
11  branches  $\leftarrow (\text{branches} \setminus \text{batch}) \cup \text{new}$ 

```

---

## 4.2 Bounding Probabilities

Our ProbabilityBounds algorithm for deriving and refining bounds on a probability is described in detail in Algorithm 4 and illustrated in Figure 1. ProbabilityBounds is a massively parallel input-splitting branch and bound procedure that leverages a bound propagation algorithm for non-probabilistic neural network verification (ComputeBounds). Since we only consider a single probability  $p_i$  as in Equation (3) in this section, we denote this probability as  $p = \mathbb{P}_{\mathbf{x}}[g_{\text{Sat}}(\mathbf{x}, \text{net}(\mathbf{x})) \geq 0]$ . ProbabilityBounds receives  $p$  and a *batch size*  $N \in \mathbb{N}$  as input. The algorithm iteratively computes  $\ell^{(t)}, u^{(t)} \in [0, 1]$ , such that  $\ell^{(t)} \leq \ell^{(t')} \leq p \leq u^{(t')} \leq u^{(t)}, \forall t, t' \in \mathbb{N}, t' \geq t$ . The following sections describe each step of ProbabilityBounds in detail.

### 4.2.1 Initialisation

Initially, we consider a single branch encompassing net’s entire input space  $\mathcal{X}$ . As in Section 3, we assume  $\mathcal{X}$  to be a bounded hyperrectangle. We use the trivial bounds  $\ell^{(0)} = 0 \leq p \leq 1 = u^{(0)}$  as initial bounds on  $p$ .

### 4.2.2 Selecting Branches

First, we select a batch of  $N \in \mathbb{N}$  branches. In the spirit of Xu et al. [65], we leverage the data parallelism of modern CPUs and GPUs to process several branches at once. In iteration  $t = 1$ , the batch only contains the branch  $\mathcal{X}$ . Which branches we select determines how fast we obtain tight bounds on  $p$ . We propose two heuristics for selecting branches:

- **SelectProb:** Inspired by FairSquare [3], this heuristic selects the  $N$  branches  $\mathcal{B}_i$  with the largest  $\mathbb{P}_{\mathbf{x}}[\mathcal{B}_i]$ . This heuristic is motivated by the observation that pruning these branches would lead to the largest improvement of  $\ell^{(t)}, u^{(t)}$ .
- **SelectProbLogBounds:** This heuristic selects the  $N$  branches  $\mathcal{B}_i$  with the largest  $\frac{\mathbb{P}_{\mathbf{x}}[\mathcal{B}_i]}{\log(e + \bar{y}_i - \underline{y}_i)}$  where  $\underline{y}, \bar{y}$  are as in ProbabilityBounds. The motivation for this heuristic is to select the branches with the largest probability while  $\underline{y}, \bar{y}$  are loose to focus on the most relevant regions of the input space, but greedily select branches that have tight bounds with the expectation that these will be pruned soon.

We compare SelectProb and SelectProbLogBounds experimentally in Appendix D. The comparison reveals that SelectProbLogBounds slightly speeds up PV compared to SelectProb.

### 4.2.3 Pruning

The next step is to prune those branches  $\mathcal{B}_j \in \text{batch}$ , for which we can determine that  $y = g_{\text{Sat}}(\mathbf{x}, \text{net}(\mathbf{x})) \geq 0$  is either certainly satisfied or certainly violated. For this, we first compute  $\underline{y} \leq g_{\text{Sat}}(\cdot, \text{net}(\cdot)) \leq \bar{y}$  for the entire batch using a sound neural network verifier like interval arithmetic, CROWN [67], or  $\alpha$ -CROWN [65]. If  $\underline{y}_j \geq 0$  ( $y \geq 0$  is certainly satisfied) or  $\bar{y}_j < 0$  ( $y \geq 0$  is certainly violated), we can prune  $\mathcal{B}_j$  analogously to Algorithm 2. We collect the branches with  $\underline{y}_j \geq 0$  in the set  $\mathcal{X}_{\text{sat}}^{(t)}$  and the branches with  $\bar{y}_j < 0$  in  $\mathcal{X}_{\text{viol}}^{(t)}$ , where  $t \in \mathbb{N}$  is the current iteration.

### 4.2.4 Updating Bounds

Let  $\hat{\mathcal{X}}_{\text{sat}}^{(t)} = \bigcup_{t'=1}^t \mathcal{X}_{\text{sat}}^{(t')}$  and  $\hat{\mathcal{X}}_{\text{viol}}^{(t)} = \bigcup_{t'=1}^t \mathcal{X}_{\text{viol}}^{(t')}$ , where  $t \in \mathbb{N}$  is the current iteration. Then,  $\ell^{(t)} = \mathbb{P}_{\mathbf{x}}[\hat{\mathcal{X}}_{\text{sat}}^{(t)}] \leq p$ . Similarly,  $\ell^{(t)} = \mathbb{P}_{\mathbf{x}}[\hat{\mathcal{X}}_{\text{viol}}^{(t)}] \leq \mathbb{P}_{\mathbf{x}}[f_{\text{Sat}}(\mathbf{x}, \text{net}(\mathbf{x})) < 0] = 1 - p$ . Therefore,  $1 - \ell^{(t)} =$



$u^{(t)} \geq p$ . Practically, we only have to maintain the current bounds  $\ell^{(t)}$  and  $u^{(t)}$  instead of the sets  $\hat{\mathcal{X}}_{sat}^{(t)}$  and  $\hat{\mathcal{X}}_{viol}^{(t)}$ .

Because  $\hat{\mathcal{X}}_{sat}^{(t)}$  and  $\hat{\mathcal{X}}_{viol}^{(t)}$  are a union of disjoint hyperrectangles, exactly computing  $\mathbb{P}_{\mathbf{x}}[\hat{\mathcal{X}}_{sat}^{(t)}]$  and  $\mathbb{P}_{\mathbf{x}}[\hat{\mathcal{X}}_{viol}^{(t)}]$  is feasible for a large class of probability distributions, including discrete, uniform, and univariate continuous distributions, as well as Mixture Models and Bayesian Networks of such distributions, but not, for example, multivariate normal distributions. Practically, one must also accommodate floating point errors in these computations. While we do not address this in this paper, our approach can be extended to this end.

ProbabilityBounds now reports the refined bounds  $\ell^{(t)} \leq p \leq u^{(t)}$  to PV, which applies interval arithmetic to determine whether net is feasible for the probabilistic verification problem. If this remains inconclusive, we proceed with splitting the selected branches.

#### 4.2.5 Splitting

Splitting refines a branch  $\mathcal{B} = [\underline{\mathbf{x}}, \bar{\mathbf{x}}]$  by selecting a dimension  $d \in \{1, \dots, n\}$  to split. We first describe how  $d$  is split before discussing how to select  $d$ . A dimension can encode several types of variables. We consider continuous variables, such as normalised pixel values, integer variables, such as age, and dimensions containing one indicator of a one-hot encoded categorical variable like gender. The type of variable encoded in  $d$  determines how we split  $d$ .

- For a continuous variable, we bisect  $\mathcal{B}$  along  $d$  resulting in two new branches  $[\underline{\mathbf{x}}', \bar{\mathbf{x}}']$  and  $[\underline{\mathbf{x}}'', \bar{\mathbf{x}}'']$ . Concretely,  $\underline{\mathbf{x}}'_{d'} = \underline{\mathbf{x}}''_{d'} = \underline{\mathbf{x}}_{d'}$  and  $\bar{\mathbf{x}}'_{d'} = \bar{\mathbf{x}}''_{d'} = \bar{\mathbf{x}}_{d'}$  for all  $d' \in \{1, \dots, n\} \setminus \{d\}$  while  $\bar{\mathbf{x}}'_d = \underline{\mathbf{x}}'_d = (\underline{\mathbf{x}}_d + \bar{\mathbf{x}}_d)/2$ ,  $\underline{\mathbf{x}}'_d = \underline{\mathbf{x}}_d$ , and  $\bar{\mathbf{x}}''_d = \bar{\mathbf{x}}_d$ .
- For integer variables, we bisect along  $d$  to obtain  $[\underline{\mathbf{x}}', \bar{\mathbf{x}}']$ ,  $[\underline{\mathbf{x}}'', \bar{\mathbf{x}}'']$  and round  $\bar{\mathbf{x}}'_d$  to the next smaller integer while rounding  $\underline{\mathbf{x}}''_d$  to the next larger integer.
- For a one-hot encoded categorical variable  $A$  encoded in the dimensions  $D \in \{1, \dots, n\}$  with  $d \in D$ , we create one split where  $A$  is equal to the category represented by  $d$  and one where  $A$  is different from this category. Formally,  $\underline{\mathbf{x}}'_d = \bar{\mathbf{x}}'_d = 1$  and  $\underline{\mathbf{x}}'_{d'} = \bar{\mathbf{x}}'_{d'} = 0$  for  $d' \in D \setminus \{d\}$  defines  $[\underline{\mathbf{x}}', \bar{\mathbf{x}}']$ . For  $[\underline{\mathbf{x}}'', \bar{\mathbf{x}}'']$ , we set  $\underline{\mathbf{x}}''_d = \bar{\mathbf{x}}''_d = 0$  and leave the remaining values as they are in  $\underline{\mathbf{x}}$  and  $\bar{\mathbf{x}}^1$ .

In any case, we need to ensure not to select  $d$  if  $\underline{\mathbf{x}}_d = \bar{\mathbf{x}}_d$ . We introduce two heuristics for selecting a dimension:

- LongestEdge: This well-known heuristic [15] selects the dimension  $d$  with the largest *edge length*  $\bar{\mathbf{x}}_d - \underline{\mathbf{x}}_d$ .
- BaBSB: We use a variant of the BaBSB heuristic of Bunel et al. [15]. The idea of BaBSB is to estimate the improvement in bounds that splitting dimension  $d$  yields by using a yet less expensive technique than ComputeBounds. Our variant of BaBSB uses interval arithmetic, assuming that we use CROWN or  $\alpha$ -CROWN for ComputeBounds. Let  $[\underline{\mathbf{x}}^{(d,1)}, \bar{\mathbf{x}}^{(d,1)}]$  and  $[\underline{\mathbf{x}}^{(d,2)}, \bar{\mathbf{x}}^{(d,2)}]$  be the two new branches originating from splitting dimension  $d \in \{1, \dots, n\}$  and let  $\underline{y}^{(d,1)}, \bar{y}^{(d,1)}, \underline{y}^{(d,2)}, \bar{y}^{(d,2)}$  be the bounds that interval arithmetic computes on  $g_{\text{Sat}}(\cdot, \text{net}(\cdot))$  for these branches. Our BaBSB selects  $d = \arg \max_{d \in \{1, \dots, n\}} \tilde{y}^{(d)}$ , where  $\tilde{y}^{(d)} = \max(\max(\underline{y}^{(d,1)}, \underline{y}^{(d,2)}), -\min(\bar{y}^{(d,1)}, \bar{y}^{(d,2)}))$ .

While LongestEdge is more theoretically accessible, BaBSB is practically advantageous, as discussed in Appendix D.

<sup>1</sup>This splitting procedure eventually creates a new branch where all dimensions are set to zero. This branch has zero probability and can be discarded immediately.

## 5 Theoretical Analysis

In this section, we prove that PV is a sound probabilistic verification algorithm when instantiated with a suitable ComputeBounds procedure. We also prove that PV instantiated with SelectProb, LongestEdge, and interval arithmetic for ComputeBounds is complete under mild assumptions on the probabilistic verification problem. Soundness and completeness are defined in Definition 2. As in Section 4.2, we omit index and superscripts when considering only a single probability  $p = \mathbb{P}_{\mathbf{x}}[g_{\text{Sat}}(\mathbf{x}, \text{net}(\mathbf{x})) \geq 0]$ .

### 5.1 Soundness

First, we prove that ProbabilityBounds produces sound bounds on  $p$  when using a sound ComputeBounds procedure, that is, a procedure that computes valid bounds, such as interval arithmetic or CROWN [67]. The soundness of PV then follows immediately.

**Theorem 1** (Sound Bounds). *Let  $N \in \mathbb{N}$  be a batch size and assume ComputeBounds produces valid bounds. Let  $((\ell^{(t)}, u^{(t)}))_{t \in \mathbb{N}}$  be the iterates of ProbabilityBounds( $\mathbb{P}_{\mathbf{x}}[g_{\text{Sat}}(\mathbf{x}, \text{net}(\mathbf{x})) \geq 0]$ ,  $N$ ). It holds that  $\ell^{(t)} \leq \mathbb{P}_{\mathbf{x}}[g_{\text{Sat}}(\mathbf{x}, \text{net}(\mathbf{x})) \geq 0] \leq u^{(t)}$  for all  $t \in \mathbb{N}$ .*

*Proof.* Let  $t \in \mathbb{N}$  and let  $\mathcal{X}_{\text{sat}}^{(t)}$  and  $\mathcal{X}_{\text{viol}}^{(t)}$  be as in Algorithm 4. ProbabilityBounds computes  $\ell^{(t)}$  as the total probability of all previously pruned satisfied branches  $\hat{\mathcal{X}}_{\text{sat}}^{(t)} = \bigcup_{t'=1}^t \mathcal{X}_{\text{sat}}^{(t')}$ . Similarly,  $u^{(t)} = 1 - \hat{k}^{(t)}$  where  $\hat{k}^{(t)}$  is the total probability of all previously pruned violated branches  $\hat{\mathcal{X}}_{\text{viol}}^{(t)} = \bigcup_{t'=1}^t \mathcal{X}_{\text{viol}}^{(t')}$ . Since we assumed that ComputeBounds produces valid bounds, Prune only prunes branches that are actually satisfied or violated. Therefore,  $\hat{\mathcal{X}}_{\text{sat}}^{(t)} \subseteq \{\mathbf{x} \in \mathcal{X} \mid g_{\text{Sat}}(\mathbf{x}, \text{net}(\mathbf{x})) \geq 0\}$  and  $\hat{\mathcal{X}}_{\text{viol}}^{(t)} \subseteq \{\mathbf{x} \in \mathcal{X} \mid g_{\text{Sat}}(\mathbf{x}, \text{net}(\mathbf{x})) < 0\}$ . From this, it follows directly that

$$\begin{aligned} \ell^{(t)} &= \mathbb{P}_{\mathbf{x}} \left[ \hat{\mathcal{X}}_{\text{sat}}^{(t)} \right] \leq \mathbb{P}_{\mathbf{x}} [g_{\text{Sat}}(\mathbf{x}, \text{net}(\mathbf{x})) \geq 0] \\ \hat{k}^{(t)} &= \mathbb{P}_{\mathbf{x}} \left[ \hat{\mathcal{X}}_{\text{viol}}^{(t)} \right] \leq \mathbb{P}_{\mathbf{x}} [g_{\text{Sat}}(\mathbf{x}, \text{net}(\mathbf{x})) < 0], \end{aligned}$$

which implies  $u^{(t)} = 1 - \hat{k}^{(t)} \geq 1 - \mathbb{P}_{\mathbf{x}}[g_{\text{Sat}}(\mathbf{x}, \text{net}(\mathbf{x})) < 0] = \mathbb{P}_{\mathbf{x}}[g_{\text{Sat}}(\mathbf{x}, \text{net}(\mathbf{x})) \geq 0]$ . This shows that ProbabilityBounds is sound.  $\square$

**Corollary 1** (Soundness). *PV is sound when using a ComputeBounds procedure that computes valid bounds.*

*Proof.* Corollary 1 follows from Theorem 1 and the soundness of interval arithmetic [42, Theorem 5.1]<sup>2</sup>.  $\square$

### 5.2 Completeness

We study the completeness of PV. Concretely, we prove that PV instantiated with SelectProb, interval arithmetic for ComputeBounds, and LongestEdge is complete under a mildly restrictive condition on Equation (3).

**Assumption 1.** Let  $v, f_{\text{Sat}}, g_{\text{Sat}}^{(i)}$ , and  $\mathbf{x}^{(i)}$  be as in Equation (3). Assume  $f_{\text{Sat}}(p_1, \dots, p_v) \neq 0$  and  $\forall i \in \{1, \dots, v\} : \mathbb{P}_{\mathbf{x}^{(i)}}[g_{\text{Sat}}^{(i)}(\mathbf{x}^{(i)}, \text{net}(\mathbf{x}^{(i)})) = 0] = 0$ .

<sup>2</sup>We include relevant theorems from Moore et al. [42] in Appendix B.2 for reference.

To prove the completeness of PV, we first establish that ProbabilityBounds produces a sequence of lower and upper bounds that converge towards each other. Intuitively, we require Assumption 1 since converging bounds on  $f_{\text{Sat}}(p_1, \dots, p_n)$  are insufficient for proving  $f_{\text{Sat}}(p_1, \dots, p_n) \geq 0$  if  $f_{\text{Sat}}(p_1, \dots, p_n) = 0$  [3]. However, excluding  $f_{\text{Sat}}(p_1, \dots, p_n) = 0$  is only mildly restrictive as we can always tighten the constraint to  $f_{\text{Sat}}(p_1, \dots, p_n) \geq \varepsilon$  for an arbitrarily small  $\varepsilon > 0$ . The second assumption  $\mathbb{P}_{\mathbf{x}}[g_{\text{Sat}}(\mathbf{x}, \text{net}(\mathbf{x})) = 0] = 0$  is only mildly restrictive for similar reasons. In particular, we can tighten  $\mathbb{P}_{\mathbf{x}}[g_{\text{Sat}}(\mathbf{x}, \text{net}(\mathbf{x})) \geq 0]$  to  $\mathbb{P}_{\mathbf{x}}[g_{\text{Sat}}(\mathbf{x}, \text{net}(\mathbf{x})) \geq \varepsilon]$  for  $\varepsilon > 0$  such that  $\mathbb{P}_{\mathbf{x}}[g_{\text{Sat}}(\mathbf{x}, \text{net}(\mathbf{x})) = \varepsilon] = 0$ . Such a  $\varepsilon > 0$  exists because  $\mathbb{P}_{\mathbf{x}}[g_{\text{Sat}}(\mathbf{x}, \text{net}(\mathbf{x})) = 0] = 0$  means that the satisfaction boundary has positive volume, but any neural network has only finitely many flat regions that can produce a satisfaction boundary of positive volume.

**Lemma 1** (Converging Probability Bounds). *Let  $N \in \mathbb{N}$  be a batch size. Let  $((\ell^{(t)}, u^{(t)}))_{t \in \mathbb{N}}$  be the iterates of ProbabilityBounds( $\mathbb{P}_{\mathbf{x}}[g_{\text{Sat}}(\mathbf{x}, \text{net}(\mathbf{x})) \geq 0]$ ,  $N$ ) instantiated with SelectProb, interval arithmetic for ComputeBounds and LongestEdge. Assume  $\mathbb{P}_{\mathbf{x}}[g_{\text{Sat}}(\mathbf{x}, \text{net}(\mathbf{x})) = 0] = 0$  as in Assumption 1. Then,*

$$\lim_{t \rightarrow \infty} \ell^{(t)} = \lim_{t \rightarrow \infty} u^{(t)} = \mathbb{P}_{\mathbf{x}}[g_{\text{Sat}}(\mathbf{x}, \text{net}(\mathbf{x})) \geq 0].$$

**Purely Discrete Input Spaces.** In the following, we assume that the input space  $\mathcal{X}$  of net contains at least one continuous variable. Otherwise,  $\mathcal{X}$  contains only finitely many discrete values. This implies that ProbabilityBounds eventually reaches an iteration where no branch can be split further. However, in this iteration, all branches are points in the input space, for which interval arithmetic computes  $\underline{\mathbf{y}} = \bar{\mathbf{y}}$  [42, see Appendix B.2]. In turn, this implies that all branches are pruned, making ProbabilityBounds complete.

We require the following intermediate result for proving Lemma 1. We write  $\mathcal{B} \rightsquigarrow \mathcal{B}_t$  if  $\mathcal{B}_t$  is a branch in iteration  $t$  of ProbabilityBounds that originates from splitting  $\mathcal{B}$ , meaning that  $\mathcal{B}_t \subset \mathcal{B}$ .

**Lemma 2.** *Let  $N \in \mathbb{N}$ . ProbabilityBounds instantiated as in Lemma 1 satisfies*

$$\forall t \in \mathbb{N} : \forall \mathcal{B} \in \text{branches}^{(t)} : \mathbb{P}_{\mathbf{x}}[\mathcal{B}] > 0 \implies \exists t' \geq t : \mathcal{B} \in \text{SelectProb}(\text{branches}^{(t')}, N),$$

where  $\text{branches}^{(t)}$  is the value of the branches variable of ProbabilityBounds in iteration  $t$ .

*Proof.* Let  $N \in \mathbb{N}$  and let  $\mathcal{B} \notin \text{SelectProb}(\text{branches}^{(t)}, N)$  in iteration  $t \in \mathbb{N}$  of ProbabilityBounds with  $\mathbb{P}_{\mathbf{x}}[\mathcal{B}] > 0$ . There are at least  $N$  branches  $\mathcal{B}'_t$  in iteration  $t$  with  $\mathbb{P}_{\mathbf{x}}[\mathcal{B}'_t] \geq \mathbb{P}_{\mathbf{x}}[\mathcal{B}]$ . We show

$$\exists t' > t : \forall \mathcal{B}'_t, \mathbb{P}_{\mathbf{x}}[\mathcal{B}'_t] \geq \mathbb{P}_{\mathbf{x}}[\mathcal{B}] : \underbrace{\forall \mathcal{B}'_{t'}, \mathcal{B}'_t \rightsquigarrow \mathcal{B}'_{t'} : \mathbb{P}_{\mathbf{x}}[\mathcal{B}'_{t'}] < \mathbb{P}_{\mathbf{x}}[\mathcal{B}]}_{(*)}. \quad (5)$$

Let  $\mathcal{B}'_t$  be a branch in iteration  $t$  with  $\mathbb{P}_{\mathbf{x}}[\mathcal{B}'_t] \geq \mathbb{P}_{\mathbf{x}}[\mathcal{B}]$ . We first show that there is an iteration  $t' > t$  such that  $(*)$  holds for  $\mathcal{B}'_t$ .

First of all, if  $\mathcal{B}'_t$  is pruned by ProbabilityBounds in iteration  $t$ , then there are no new branches originating from  $\mathcal{B}'_t$ , so that  $(*)$  holds vacuously. Otherwise, ProbabilityBounds splits  $\mathcal{B}'_t$ .

Without loss of generality, assume that the dimension selected for splitting encodes a continuous variable. This does not harm generality since discrete variables in a bounded input space can only be split finitely often and will, therefore, eventually become unavailable for splitting. Since we split continuous variables by bisection, we have that the volume of all branches  $\mathcal{B}'_{t'}$  originating from  $\mathcal{B}'_t$  decreases towards zero as  $t'$  increases.

As stated in Section 3, we assume that all continuous random variables admit a probability density function. This implies that the probability in all branches  $\mathcal{B}'_{t'}$  originating from  $\mathcal{B}'_t$  decreases towards zero as the volume decreases towards zero. Therefore, there is a  $t'$ , such that  $(*)$  is satisfied for  $\mathcal{B}'_t$ . Since there are only finitely many branches in any iteration of ProbabilityBounds, the above implies that Equation (5) is satisfied. In turn, this directly implies that  $\mathcal{B}$  is eventually selected by ProbabilityBounds, proving Lemma 2.  $\square$

*Proof of Lemma 1.* We first prove that  $\lim_{t \rightarrow \infty} \ell^{(t)} = \mathbb{P}_{\mathbf{x}}[g_{\text{Sat}}(\mathbf{x}, \text{net}(\mathbf{x})) \geq 0]$ . The convergence of the upper bound,  $\lim_{t \rightarrow \infty} u^{(t)} = \mathbb{P}_{\mathbf{x}}[g_{\text{Sat}}(\mathbf{x}, \text{net}(\mathbf{x})) \geq 0]$  follows with a similar argument.

Let  $\mathcal{X}_{\text{sat}}^* = \{\mathbf{x} \in \mathcal{X} \mid g_{\text{Sat}}(\mathbf{x}, \text{net}(\mathbf{x})) > 0\}$ , where  $\mathcal{X}$  is the input space of `net`. Note that  $\mathbb{P}_{\mathbf{x}}[\mathcal{X}_{\text{sat}}^*] = \mathbb{P}_{\mathbf{x}}[\{\mathbf{x} \in \mathcal{X} \mid g_{\text{Sat}}(\mathbf{x}, \text{net}(\mathbf{x})) \geq 0\}]$  due to Assumption 1. Further, let  $\hat{\mathcal{X}}_{\text{sat}}^{(t)}$  be as in the proof of Theorem 1 and recall  $\ell^{(t)} = \mathbb{P}_{\mathbf{x}}[\hat{\mathcal{X}}_{\text{sat}}^{(t)}]$ .

First, we give an argument why the limit  $\lim_{t \rightarrow \infty} \ell^{(t)}$  exists. Due to Theorem 1,  $\ell^{(t)}$  is bounded from above. Furthermore,  $\ell^{(t)}$  is non-decreasing in  $t$  since `ProbabilityBounds` only adds elements to  $\hat{\mathcal{X}}_{\text{sat}}^{(t)}$ . Therefore,  $\lim_{t \rightarrow \infty} \ell^{(t)}$  exists. Given this, we now show

$$\begin{aligned}
& \ell^{(t)} \xrightarrow[t \rightarrow \infty]{} \mathbb{P}_{\mathbf{x}}[g_{\text{Sat}}(\mathbf{x}, \text{net}(\mathbf{x})) \geq 0] \\
\iff & \mathbb{P}_{\mathbf{x}}[\hat{\mathcal{X}}_{\text{sat}}^{(t)}] \xrightarrow[t \rightarrow \infty]{} \mathbb{P}_{\mathbf{x}}[\mathcal{X}_{\text{sat}}^*] \\
\iff & \mathbb{P}_{\mathbf{x}}[\hat{\mathcal{X}}_{\text{sat}}^{(t)}] - \mathbb{P}_{\mathbf{x}}[\mathcal{X}_{\text{sat}}^*] \xrightarrow[t \rightarrow \infty]{} 0 \\
\iff & \mathbb{P}_{\mathbf{x}}[\mathcal{X}_{\text{sat}}^* \setminus \hat{\mathcal{X}}_{\text{sat}}^{(t)}] \xrightarrow[t \rightarrow \infty]{} 0. \tag{6}
\end{aligned}$$

We prove Equation (6) by showing that  $\tilde{\mathcal{X}}_{\text{sat}}^{(t)} = \mathcal{X}_{\text{sat}}^* \setminus \hat{\mathcal{X}}_{\text{sat}}^{(t)}$  has diminishing volume. Since we assumed the input space to contain at least one continuous variable and assumed all continuous random variables to admit a density function, diminishing volume implies diminishing probability.

With the goal of obtaining a contradiction, assume  $\lim_{t \rightarrow \infty} \text{vol}(\tilde{\mathcal{X}}_{\text{sat}}^{(t)}) > 0$ , where `vol` denotes the volume of a set. Let  $t \in \mathbb{N}$ . Since the branches maintained by `ProbabilityBounds` form a partition of the input space, there is a branch  $\mathcal{B}_t$  in iteration  $t$  of `ProbabilityBounds` such that  $\tilde{\mathcal{X}}_{\text{sat}}^{(t)} \cap \mathcal{B}_t \neq \emptyset$ .

A central argument in the following is that `LongestEdge` eventually splits every dimension since splitting decreases the edge length  $\bar{\mathbf{x}}_d - \underline{\mathbf{x}}_d$  of the dimension  $d$  being split. Due to this and due to Lemma 2, we eventually obtain  $\mathcal{B}_{t'}$  in iteration  $t' > t$  with  $\mathcal{B}_{t'} \subseteq \tilde{\mathcal{X}}_{\text{sat}}^{(t)} \cap \mathcal{B}_t$ . Also, since `LongestEdge` eventually splits every dimension, Theorem 6.1 of Moore et al. [42] applies, which states that the bounds  $\underline{y} \leq g_{\text{Sat}}(\mathbf{x}, \text{net}(\mathbf{x})) \leq \bar{y}$  produced by interval arithmetic converge towards  $g_{\text{Sat}}(\mathbf{x}, \text{net}(\mathbf{x}))$ . However, this implies that there is an iteration  $t'' > t'$  in which `ProbabilityBounds` considers a branch  $\mathcal{B}_{t''} \subset \tilde{\mathcal{X}}_{\text{sat}}^{(t)}$  for which  $\underline{y} > 0$ , which means that `ProbabilityBounds` prunes  $\mathcal{B}_{t''}$ . This contradicts the construction of  $\tilde{\mathcal{X}}_{\text{sat}}^{(t)}$ .

With this contradiction, we have shown  $\lim_{t \rightarrow \infty} \ell^{(t)} = \mathbb{P}_{\mathbf{x}}[g_{\text{Sat}}(\mathbf{x}, \text{net}(\mathbf{x})) \geq 0]$ . Convergence of the upper bound  $u^{(t)}$  follows from an analogous argument on  $k^{(t)}$  as in the proof of Theorem 1 where  $u^{(t)} = 1 - k^{(t)}$ . This establishes Lemma 1.  $\square$

**Theorem 2 (Completeness).** *When instantiated with `ProbabilityBounds` as in Lemma 1, PV is complete for verification problems satisfying Assumption 1.*

*Proof.* Let `net`,  $f_{\text{Sat}}^{(1)}, g_{\text{Sat}}^{(1)}, \dots, g_{\text{Sat}}^{(v)}$  be as in Equation (3). First, consider  $f_{\text{Sat}}(p_1, \dots, p_v) > 0$ . As a consequence of Theorem 6.1 of Moore et al. [42] and Lemma 1, the bounds  $\ell \leq f_{\text{Sat}}(p_1, \dots, p_v) \leq u$  produced by interval arithmetic converge towards  $f_{\text{Sat}}(p_1, \dots, p_v)$ . This implies that eventually  $\ell > 0$ , meaning that PV eventually proves  $f_{\text{Sat}}(p_1, \dots, p_v) \geq 0$ .

If  $f_{\text{Sat}}(p_1, \dots, p_v) < 0$  we eventually obtain  $u < 0$  with the same argument as above. Since  $u < 0$  disproves  $f_{\text{Sat}}(p_1, \dots, p_v) \geq 0$ , PV is complete for probabilistic verification problems satisfying Assumption 1.  $\square$

## 6 Experiments

We apply PV (Algorithm 3) to verify the demographic parity fairness notion, count the number of safety violations of a neural network controller in a safety-critical system, and quantify the

Benchmark	Input Dimension	Input Distributions	Network Size	Source
FairSquare	2–3	independent 2 Bayesian Networks	$1 \times 1, 1 \times 2$	[3]
ACAS Xu	5	uniform	$6 \times 50$	[34]
MiniACSIncome	1–8	Bayesian Network	$1 \times 10$ – $10000$ $1 \times 10 - 10 \times 10$	Own

Table 1: **Benchmarks.** Network size is the size of the neural network given as #layers $\times$ layer size.

robustness of a neural network. We use the SelectProbLogBounds and BaBSB heuristics and use CROWN [67] for ComputeBounds. Table 1 gives an overview of the benchmarks considered in this section. All verification problems are defined formally in Appendix A.

As our results show, PV outpaces the probabilistic verification algorithms FairSquare [3] and SpaceScanner [19]. Additionally, we show that ProbabilityBounds compares favourably to the ProVe\_SLR [40] and  $\varepsilon$ -ProVe [39] algorithms for #DNN verification [38], which corresponds to probabilistic verification with uniformly distributed inputs.

While no code is publicly available for SpaceScanner, running ProVe\_SLR is very computationally expensive. To enable a faithful comparison, we run our experiments on less powerful hardware (HW1) compared to the hardware used by Converse et al. [19] and Marzari et al. [40] and compare the runtime of our algorithms to the runtimes reported by these authors. To obtain comparable runtimes across the experiments in this section, we run all experiments on HW1. The results of FairSquare and  $\varepsilon$ -ProVe were similarly obtained on HW1. Additional experiments on more powerful hardware are contained in Appendix D

To test the limits of PV, we introduce a new, challenging benchmark: MiniACSIncome is based on the ACSIncome dataset [20] and consists of datasets of varying input dimensionality, probability distributions for these datasets, and neural networks of varying sizes. PV solves seven of eight instances in MiniACSIncome within an hour.

**Hardware and Implementation.** We implement PV in Python, leveraging PyTorch [48] and auto\_LiRPA [65]. Our code and benchmarks are available at <https://github.com/sen-uni-kn/probspecs>. We run all experiments on a desktop running Ubuntu 22.04 with an Intel i7-4820K CPU, 32 GB of memory, and no GPU (HW1). Appendix C.1 compares our hardware to the hardware used by Converse et al. [19] and Marzari et al. [40].

## 6.1 FairSquare Benchmark

Albarghouthi et al. [3] evaluate their FairSquare algorithm on an application derived from the Adult [1] dataset. In particular, they verify the fairness of three small neural networks with respect to a person’s sex under three different distributions of the network input: a distribution of entirely independent univariate variables and two Bayesian Networks. We replicate these experiments to compare PV to FairSquare.

The FairSquare benchmark assumes that all input variables except ‘sex’ are unbounded, although some variables, like a person’s age, have natural bounds. To apply PV, we set the bounds of the input space such that the cumulative distribution functions of the input variables are 0 at the lower bound and 1 at the upper bound, up to machine precision.

Table 2 contains the results of our experiment. Our verification results match the results of FairSquare. Regarding runtime, PV significantly outperforms FairSquare. In particular, PV verifies NN<sub>3,2</sub> in several seconds, while FairSquare requires more than seven minutes for the independent input distribution and exceeds the time budget of 15 minutes for the Bayesian network input

Benchmark Instance		Runtime (s)		
net	$\mathbb{P}_x$	PV (Ours)	FairSquare [3]	Fair?
NN <sub>2,1</sub>	independent	1.3	2.1	✓
NN <sub>2,1</sub>	Bayes Net 1	2.2	75.5	✓
NN <sub>2,1</sub>	Bayes Net 2	3.6	50.5	✓
NN <sub>2,2</sub>	independent	1.8	4.2	✓
NN <sub>2,2</sub>	Bayes Net 1	3.3	33.3	✓
NN <sub>2,2</sub>	Bayes Net 2	4.9	58.6	✓
NN <sub>3,2</sub>	independent	2.2	450.5	✓
NN <sub>3,2</sub>	Bayes Net 1	4.4	TO	✓
NN <sub>3,2</sub>	Bayes Net 2	6.9	TO	✓

Table 2: **FairSquare Benchmark.** NN<sub>*i,j*</sub> denotes a neural network with *i* inputs and a single hidden layer of *j* neurons. ‘TO’ indicates timeout (900s).

distributions. A comparison with FairSquare on an extended set of benchmarks is contained in Appendix C.2.

## 6.2 ACAS Xu Safety

The ACAS Xu networks [34] are a suite of 45 networks, together forming a collision avoidance system for crewless aircraft. We reproduce the ACAS Xu #DNN verification [38] experiments of Marzari et al. [40]. In particular, we seek to *quantify* the number of violations (violation rate) of the ACAS Xu networks that violate the property  $\phi_2$  introduced by Katz et al. [34]. This corresponds to computing bounds on Equation (2) under a uniform distribution of  $x$ .

We compare ProbabilityBounds (Algorithm 4) to the ProVe\_SLR and  $\varepsilon$ -ProVe algorithms for #DNN verification. ProVe\_SLR [40] computes the violation rate exactly, while  $\varepsilon$ -ProVe [39] computes an upper bound on the violation rate that is sound with a certain probability. In contrast, ProbabilityBounds provides sound bounds on the violation rate at any time during its execution. Therefore, we can run ProbabilityBounds only for a particular time budget or abort ProbabilityBounds when the bounds become sufficiently tight.

Table 3 compares ProbabilityBounds (Algorithm 4) with ProVe\_SLR and  $\varepsilon$ -ProVe for the ACAS Xu property  $\phi_2$  [34] and the networks investigated by Marzari et al. [40]. For all three networks, ProbabilityBounds can tighten the bounds to a margin of less than 0.007 within one hour, while ProVe\_SLR requires at least four hours to compute the exact violation rate. In comparison to  $\varepsilon$ -ProVe, ProbabilityBounds produces tighter sound upper bounds within 10 seconds in two of three cases, while  $\varepsilon$ -ProVe requires at least 57 seconds to derive a probably sound upper bound for these cases. The extended comparison in Appendix C.3 reveals that, in 13 from a total of 36 cases, ProbabilityBounds computes tighter sound bounds faster than  $\varepsilon$ -ProVe computes a *probably sound* upper bound.

## 6.3 ACAS Xu Robustness

We replicate the experiments of Converse et al. [19] who apply SpaceScanner to quantify the robustness of ACAS Xu network  $N_{1,1}$  [34] under adversarial perturbations. As Converse et al. [19], we consider 25 reference inputs — five for each class — and allow these reference inputs to be perturbed in the first two dimensions by at most 5% of the diameter of the input space in the respective dimension. To compute bounds on the output distribution, we bound the probability of each of the five ACAS Xu classes for each of the 25 inputs. Since the ACAS Xu training data is not publicly available, we sample the reference inputs randomly.



net	ProbabilityBounds (Ours)			ProVe_SLR [40]		$\epsilon$ -ProVe [39]	
	10s $\ell, u$	1m $\ell, u$	1h $\ell, u$	Exact VR	Rt	99.9% confid. $u$ Rt	
$N_{4,3}$	0.19%, 2.90%	0.62%, 2.28%	1.12%, 1.75%	1.43%	8h 46m	3.61%	64.5s
$N_{4,9}$	0.00%, 3.39%	0.00%, 1.65%	0.08%, 0.30%	0.15%	12h 21m	0.73%	19.5s
$N_{5,8}$	0.95%, 4.12%	1.58%, 3.11%	1.97%, 2.57%	2.20%	4h 35m	4.52%	57.0s

Table 3: **Comparison of ProbabilityBounds, ProVe\_SLR, and  $\epsilon$ -ProVe.** We run ProbabilityBounds with different time budgets (10s, 1m, 1h) and report the lower and upper bounds ( $\ell, u$ ) computed within this time budget. In contrast, ProVe\_SLR computes the exact probabilities (VR), and  $\epsilon$ -ProVe computes a 99.9% confidence (confid.) upper bound. The runtimes (Rt) of ProVe\_SLR are taken from Marzari et al. [40].

The mean runtime of ProbabilityBounds for these 125 verification problems is 18 seconds (median: 5.1s, maximum: 173.4s). Therefore, ProbabilityBounds substantially outperforms SpaceScanner, for which Converse et al. [19] report an average runtime of 33 minutes per verification problem while running their experiments on superior hardware. Appendix C.4 contains the full results.

## 6.4 MiniACSIncome

To test the limits of PV, we introduce the MiniACSIncome benchmark. MiniACSIncome is derived from the ACSIncome [20] dataset, a replacement of the Adult dataset [1] that is better suited for fair machine learning research. ACSIncome is based on US census data. The task is to predict whether a person’s yearly income exceeds \$50 000 using features such as the person’s age, sex, weekly work hours, education, etc. Our benchmark provides probabilistic verification problems of various degrees of difficulty. We apply PV to MiniACSIncome and show that it outperforms a naïve approach for solving MiniACSIncome.

**Benchmark.** To create probabilistic verification problems of increasing difficulty, we consider an increasing number of input variables from ACSIncome. The smallest instance, MiniACSIncome-1, only contains the binary ‘SEX’ variable. In contrast, the largest instance, MiniACSIncome-8, contains ‘SEX’ and seven more variables from ACSIncome, including age, education, and working hours per week. We train a neural network with a single layer of ten neurons for each MiniACSIncome- $i$ ,  $i \in \{1, \dots, 8\}$ . For MiniACSIncome-4, we additionally train deeper and wider networks to investigate the scalability of PV with respect to the network size. We fit a Bayesian Network to the MiniACSIncome-8 dataset to obtain an input distribution. We use this distribution for all MiniACSIncome- $i$  instances by taking the variables not contained in MiniACSIncome- $i$  as latent variables. The verification problem is then to verify the demographic parity of a neural network with respect to ‘SEX’ under this input distribution. Appendix C.5 contains additional details on the MiniACSIncome benchmark.

**Naïve Approach.** Since all variables in ACSIncome are discrete, we can theoretically verify the demographic parity of a neural network by enumerating all discrete values in the input space of MiniACSIncome- $i$ . However, as expected, the number of discrete values scales exponentially with the number of input variables. While MiniACSIncome-1 contains only two values, MiniACSIncome-4 already contains 38 000 values, and MiniACSIncome-8 contains 2.4 billion values. As we demonstrate next, PV can explore this space more efficiently than the naïve enumeration approach.

**Results.** Figure 2 (left) displays the runtime of PV and the naïve enumeration approach for MiniACSIncome-1 to MiniACSIncome-8. While enumeration is faster than PV for input spaces of up to three variables, where the network can be evaluated for all discrete values in one batch,

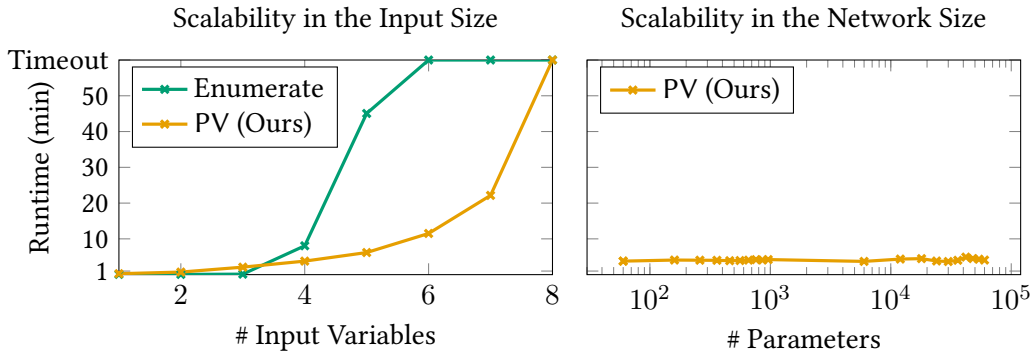


Figure 2: **MiniACSIncome Results.** The left plot depicts the runtime of PV and the naïve enumeration approach on MiniACSIncome-1 to MiniACSIncome-8 for a network of 10 neurons. The right plot depicts the runtime of PV for MiniACSIncome-4 networks of varying sizes.

enumeration falls behind PV as soon as this becomes infeasible. PV can solve MiniACSIncome for up to seven input variables in less than 30 minutes, only exceeding the timeout of one hour for MiniACSIncome-8.

**Effect of Network Size.** Figure 2 (right) displays the runtime of PV for MiniACSIncome-4 networks of various sizes. The studied networks include wide single-layer networks of up to 10 000 neurons and deep networks of up to 10 layers of 10 neurons. As the figure shows, PV is largely unaffected by the size of the MiniACSIncome-4 networks. This is unexpected since the network size indirectly determines the performance of PV through the complexity of the decision boundary. However, larger networks need not necessarily have a more complex decision boundary, and large networks do not provide a performance benefit for MiniACSIncome-4, as discussed in Appendix C.5. Thoroughly exploring the impacts of network size requires more intricate datasets for which larger networks actually provide a benefit.

## 7 Conclusion and Future Work

As Section 6 shows, our PV algorithm for the probabilistic verification of neural networks significantly outpaces existing algorithms for probabilistic verification. We obtain this speedup by recombining existing techniques for non-probabilistic neural network verification with the ideas from the FairSquare [3] fairness verifier. Our MiniACSIncome benchmark provides a testbed for future probabilistic verification algorithms.

A promising direction for such verifiers is *neuron branching* [58], which fuels the current state-of-the-art non-probabilistic neural network verifiers. However, using neuron branching for probabilistic verification is challenging because it creates non-hyperrectangular regions in the input space that are expensive to integrate over. Alternative directions include new branching and splitting heuristics, as well as switching to successively more precise bound propagation techniques during the course of ProbabilityBounds.

## References

- [1] *Adult*. UCI Machine Learning Repository. 1996. URL: <https://archive.ics.uci.edu/ml/datasets/Adult/>.
- [2] Takuya Akiba, Shotaro Sano, Toshihiko Yanase, Takeru Ohta and Masanori Koyama. ‘Optuna: A Next-generation Hyperparameter Optimization Framework’. In: *KDD*. 2019. DOI: [10.1145/3292500.3330701](https://doi.org/10.1145/3292500.3330701).

- [3] Aws Albarghouthi, Loris D’Antoni, Samuel Drews and Aditya V. Nori. ‘FairSquare: probabilistic verification of program fairness’. In: *Proc. ACM Program. Lang.* 1.OOPSLA (2017). DOI: [10.1145/3133904](https://doi.org/10.1145/3133904).
- [4] Ross Anderson, Joey Huchette, Will Ma, Christian Tjandraatmadja and Juan Pablo Vielma. ‘Strong mixed-integer programming formulations for trained neural networks’. In: *Math. Program.* 183.1 (2020). DOI: [10.1007/s10107-020-01474-5](https://doi.org/10.1007/s10107-020-01474-5).
- [5] Stanley Bak, Hoang-Dung Tran, Kerianne Hobbs and Taylor T. Johnson. ‘Improved Geometric Path Enumeration for Verifying ReLU Neural Networks’. In: *CAV (1)*. Vol. 12224. Lecture Notes in Computer Science. 2020. DOI: [10.1007/978-3-030-53288-8\\_4](https://doi.org/10.1007/978-3-030-53288-8_4).
- [6] Teodora Baluta, Shiqi Shen, Shweta Shinde, Kuldeep S. Meel and Prateek Saxena. ‘Quantitative Verification of Neural Networks and Its Security Applications’. In: *CCS*. 2019. DOI: [10.1145/3319535.3354245](https://doi.org/10.1145/3319535.3354245).
- [7] Solon Barocas, Moritz Hardt and Arvind Narayanan. *Fairness and Machine Learning*. MIT Press, 2023. URL: <https://fairmlbook.org/>.
- [8] Osbert Bastani, Xin Zhang and Armando Solar-Lezama. ‘Probabilistic Verification of Fairness Properties via Concentration’. In: *Proc. ACM Program. Lang.* 3.OOPSLA (2019). DOI: [10.1145/3360544](https://doi.org/10.1145/3360544).
- [9] Fabian Bauer-Marquart, David Boetius, Stefan Leue and Christian Schilling. ‘SpecRepair: Counter-Example Guided Safety Repair of Deep Neural Networks’. In: *SPIN*. Vol. 13255. Lecture Notes in Computer Science. 2022. DOI: [10.1007/978-3-031-15077-7\\_5](https://doi.org/10.1007/978-3-031-15077-7_5).
- [10] Vaishak Belle, Andrea Passerini and Guy Van den Broeck. ‘Probabilistic Inference in Hybrid Domains by Weighted Model Integration’. In: *IJCAI*. 2015. URL: <http://ijcai.org/Abstract/15/392>.
- [11] Adel Bibi, Modar Alfadly and Bernard Ghanem. ‘Analytic Expressions for Probabilistic Moments of PL-DNN With Gaussian Input’. In: *CVPR*. 2018. DOI: [10.1109/CVPR.2018.00948](https://doi.org/10.1109/CVPR.2018.00948).
- [12] Sumon Biswas and Hriday Rajan. ‘Fairify: Fairness Verification of Neural Networks’. In: *ICSE*. 2023. DOI: [10.1109/ICSE48619.2023.00134](https://doi.org/10.1109/ICSE48619.2023.00134).
- [13] Giorgian Borca-Tasciuc, Xingzhi Guo, Stanley Bak and Steven Skiena. ‘Provable Fairness for Neural Network Models Using Formal Verification’. In: *EWAF*. Vol. 3442. CEUR Workshop Proceedings. 2023. URL: <https://ceur-ws.org/Vol-3442/paper-04.pdf>.
- [14] Christopher Brix, Stanley Bak, Changliu Liu and Taylor T. Johnson. ‘The Fourth International Verification of Neural Networks Competition (VNN-COMP 2023): Summary and Results’. In: *CoRR* abs/2312.16760 (2023). DOI: [10.48550/ARXIV.2312.16760](https://doi.org/10.48550/ARXIV.2312.16760).
- [15] Rudy Bunel, Jingyue Lu, Ilker Turkaslan, Philip H. S. Torr, Pushmeet Kohli and M. Pawan Kumar. ‘Branch and Bound for Piecewise Linear Neural Network Verification’. In: *J. Mach. Learn. Res.* 21 (2020). URL: <http://jmlr.org/papers/v21/19-468.html>.
- [16] Rudy Bunel, Alessandro De Palma, Alban Desmaison, Krishnamurthy Dvijotham, Pushmeet Kohli, Philip H. S. Torr and M. Pawan Kumar. ‘Lagrangian Decomposition for Neural Network Verification’. In: *UAI*. Vol. 124. Proceedings of Machine Learning Research. 2020. URL: <http://proceedings.mlr.press/v124/bunel20a.html>.
- [17] Nicholas Carlini and David A. Wagner. ‘Audio Adversarial Examples: Targeted Attacks on Speech-to-Text’. In: *IEEE Symposium on Security and Privacy Workshops*. 2018. DOI: [10.1109/SPW.2018.00009](https://doi.org/10.1109/SPW.2018.00009).
- [18] Chih-Hong Cheng, Georg Nührenberg and Harald Ruess. ‘Maximum Resilience of Artificial Neural Networks’. In: *ATVA*. Vol. 10482. Lecture Notes in Computer Science. 2017. DOI: [10.1007/978-3-319-68167-2\\_18](https://doi.org/10.1007/978-3-319-68167-2_18).

- [19] Hayes Converse, Antonio Filieri, Divya Gopinath and Corina S. Pasareanu. ‘Probabilistic Symbolic Analysis of Neural Networks’. In: *ISSRE*. 2020. DOI: [10.1109/ISSRE5003.2020.00023](https://doi.org/10.1109/ISSRE5003.2020.00023).
- [20] Frances Ding, Moritz Hardt, John Miller and Ludwig Schmidt. ‘Retiring Adult: New Datasets for Fair Machine Learning’. In: *NeurIPS*. 2021. URL: <https://proceedings.neurips.cc/paper/2021/hash/32e54441e6382a7fbacbbaf3c450059-Abstract.html>.
- [21] Hai Duong, Linhan Li, ThanhVu Nguyen and Matthew Dwyer. ‘A DPLL(T) Framework for Verifying Deep Neural Networks’. In: *CoRR* (2023). URL: <https://arxiv.org/abs/2307.10266>.
- [22] Cynthia Dwork, Moritz Hardt, Toniann Pitassi, Omer Reingold and Richard S. Zemel. ‘Fairness through awareness’. In: *ITCS*. 2012. DOI: [10.1145/2090236.2090255](https://doi.org/10.1145/2090236.2090255).
- [23] Javid Ebrahimi, Anyi Rao, Daniel Lowd and Dejing Dou. ‘HotFlip: White-Box Adversarial Examples for Text Classification’. In: *ACL (2)*. 2018. DOI: [10.18653/V1/P18-2006](https://doi.org/10.18653/V1/P18-2006).
- [24] European Parliament. *EU AI Act: first regulation on artificial intelligence*. 2023. URL: <https://www.europarl.europa.eu/topics/en/article/20230601STO93804/eu-ai-act-first-regulation-on-artificial-intelligence> (visited on 19/05/2024).
- [25] Michael Feldman, Sorelle A. Friedler, John Moeller, Carlos Scheidegger and Suresh Venkatasubramanian. ‘Certifying and Removing Disparate Impact’. In: *KDD*. 2015. DOI: [10.1145/2783258.2783311](https://doi.org/10.1145/2783258.2783311).
- [26] Claudio Ferrari, Mark Niklas Mueller, Nikola Jovanović and Martin Vechev. ‘Complete Verification via Multi-Neuron Relaxation Guided Branch-and-Bound’. In: *ICLR*. 2022. URL: [https://openreview.net/forum?id=l\\_amHf1oaK](https://openreview.net/forum?id=l_amHf1oaK).
- [27] Sainyam Galhotra, Yuriy Brun and Alexandra Meliou. ‘Fairness testing: testing software for discrimination’. In: *ESEC/SIGSOFT FSE*. 2017. DOI: [10.1145/3106237.3106277](https://doi.org/10.1145/3106237.3106277).
- [28] Timon Gehr, Matthew Mirman, Dana Drachler-Cohen, Petar Tsankov, Swarat Chaudhuri and Martin T. Vechev. ‘AI2: Safety and Robustness Certification of Neural Networks with Abstract Interpretation’. In: *IEEE Symposium on Security and Privacy*. 2018. URL: <https://doi.org/10.1109/SP.2018.00058>.
- [29] Dan Hendrycks and Thomas G. Dietterich. ‘Benchmarking Neural Network Robustness to Common Corruptions and Perturbations’. In: *ICLR*. 2019. URL: <https://openreview.net/forum?id=HJz6tiCqYm>.
- [30] Dan Hendrycks, Kevin Zhao, Steven Basart, Jacob Steinhardt and Dawn Song. ‘Natural Adversarial Examples’. In: *CVPR*. 2021. DOI: [10.1109/CVPR46437.2021.01501](https://doi.org/10.1109/CVPR46437.2021.01501).
- [31] Patrick Henriksen and Alessio Lomuscio. ‘DEEPSPLIT: An Efficient Splitting Method for Neural Network Verification via Indirect Effect Analysis’. In: *IJCAI*. 2021. DOI: [10.24963/ijcai.2021/351](https://doi.org/10.24963/ijcai.2021/351).
- [32] Hossein Hosseini, Baicen Xiao and Radha Poovendran. ‘Google’s Cloud Vision API is Not Robust to Noise’. In: *ICMLA*. 2017. DOI: [10.1109/ICMLA.2017.0-172](https://doi.org/10.1109/ICMLA.2017.0-172).
- [33] Guy Katz, Clark W. Barrett, David L. Dill, Kyle Julian and Mykel J. Kochenderfer. ‘Towards Proving the Adversarial Robustness of Deep Neural Networks’. In: *FVAV@iFM*. Vol. 257. EPTCS. 2017. DOI: [10.4204/EPTCS.257.3](https://doi.org/10.4204/EPTCS.257.3).
- [34] Guy Katz, Clark W. Barrett, David L. Dill, Kyle D. Julian and Mykel J. Kochenderfer. ‘Reluplex: An Efficient SMT Solver for Verifying Deep Neural Networks’. In: *CAV (1)*. Vol. 10426. Lecture Notes in Computer Science. 2017. DOI: [10.1007/978-3-319-63387-9\\_5](https://doi.org/10.1007/978-3-319-63387-9_5).
- [35] Diederik P. Kingma and Jimmy Ba. ‘Adam: A Method for Stochastic Optimization’. In: *ICLR*. 2015. DOI: [10.48550/ARXIV.1412.6980](https://doi.org/10.48550/ARXIV.1412.6980).
- [36] Matt J. Kusner, Joshua R. Loftus, Chris Russell and Ricardo Silva. ‘Counterfactual Fairness’. In: *NIPS*. 2017. URL: <https://proceedings.neurips.cc/paper/2017/hash/a486cd07e4ac3d270571622f4f316ec5-Abstract.html>.

- [37] Ailsa H. Land and Alison G. Doig. ‘An Automatic Method for Solving Discrete Programming Problems’. In: *50 Years of Integer Programming 1958-2008 - From the Early Years to the State-of-the-Art*. First published in *Econometrica* 28 (1960). 2010. DOI: [10.1007/978-3-540-68279-0\\_5](https://doi.org/10.1007/978-3-540-68279-0_5).
- [38] Luca Marzari, Davide Corsi, Ferdinando Cicalese and Alessandro Farinelli. ‘The #DNN-Verification Problem: Counting Unsafe Inputs for Deep Neural Networks’. In: *IJCAI*. 2023. DOI: [10.24963/IJCAI.2023/25](https://doi.org/10.24963/IJCAI.2023/25).
- [39] Luca Marzari, Davide Corsi, Enrico Marchesini, Alessandro Farinelli and Ferdinando Cicalese. ‘Enumerating Safe Regions in Deep Neural Networks with Provable Probabilistic Guarantees’. In: *AAAI*. 2024. DOI: [10.1609/AAAI.V38I19.30134](https://doi.org/10.1609/AAAI.V38I19.30134).
- [40] Luca Marzari, Gabriele Roncolato and Alessandro Farinelli. ‘Scaling #DNN-Verification Tools with Efficient Bound Propagation and Parallel Computing’. In: *CoRR abs/2312.05890* (2023). DOI: [10.48550/ARXIV.2312.05890](https://doi.org/10.48550/ARXIV.2312.05890).
- [41] Kiarash Mohammadi, Aishwarya Sivaraman and Golnoosh Farnadi. ‘FETA: Fairness Enforced Verifying, Training, and Predicting Algorithms for Neural Networks’. In: *EAAMO*. 2023. DOI: [10.1145/3617694.3623243](https://doi.org/10.1145/3617694.3623243).
- [42] Ramon E. Moore, R. Baker Kearfott and Michael J. Cloud. *Introduction to Interval Analysis*. SIAM, 2009. DOI: [10.1137/1.9780898717716](https://doi.org/10.1137/1.9780898717716).
- [43] Paolo Morettin, Andrea Passerini and Roberto Sebastiani. ‘A Unified Framework for Probabilistic Verification of AI Systems via Weighted Model Integration’. In: *CoRR abs/2402.04892* (2024). DOI: [10.48550/ARXIV.2402.04892](https://doi.org/10.48550/ARXIV.2402.04892).
- [44] David R. Morrison, Sheldon H. Jacobson, Jason J. Sauppe and Edward C. Sewell. ‘Branch-and-bound algorithms: A survey of recent advances in searching, branching, and pruning’. In: *Discret. Optim.* 19 (2016). DOI: [10.1016/j.disopt.2016.01.005](https://doi.org/10.1016/j.disopt.2016.01.005).
- [45] Mark Niklas Müller, Christopher Brix, Stanley Bak, Changliu Liu and Taylor T. Johnson. ‘The Third International Verification of Neural Networks Competition (VNN-COMP 2022): Summary and Results’. In: *CoRR abs/2212.10376* (2022). DOI: [10.48550/arXiv.2212.10376](https://doi.org/10.48550/arXiv.2212.10376).
- [46] Mark Niklas Müller, Gleb Makarchuk, Gagandeep Singh, Markus Püschel and Martin T. Vechev. ‘PRIMA: general and precise neural network certification via scalable convex hull approximations’. In: *Proc. ACM Program. Lang.* 6.POPL (2022). URL: <https://doi.org/10.1145/3498704>.
- [47] Alessandro De Palma, Harkirat S. Behl, Rudy Bunel, Philip H. S. Torr and M. Pawan Kumar. ‘Scaling the Convex Barrier with Active Sets’. In: *ICLR*. 2021. URL: <https://openreview.net/forum?id=uQfOy7LrlTR>.
- [48] Adam Paszke, Sam Gross, Francisco Massa, Adam Lerer, James Bradbury, Gregory Chanan, Trevor Killeen, Zeming Lin, Natalia Gimelshein, Luca Antiga, Alban Desmaison, Andreas Köpf, Edward Yang, Zachary DeVito, Martin Raison, Alykhan Tejani, Sasank Chilamkurthy, Benoit Steiner, Lu Fang, Junjie Bai and Soumith Chintala. ‘PyTorch: An Imperative Style, High-Performance Deep Learning Library’. In: *NeurIPS*. 2019. URL: <https://proceedings.neurips.cc/paper/2019/hash/bdbca288fee7f92f2bfa9f7012727740-Abstract.html>.
- [49] Dino Pedreschi, Salvatore Ruggieri and Franco Turini. ‘Discrimination-aware data mining’. In: *KDD*. 2008. DOI: [10.1145/1401890.1401959](https://doi.org/10.1145/1401890.1401959).
- [50] Luca Pulina and Armando Tacchella. ‘An Abstraction-Refinement Approach to Verification of Artificial Neural Networks’. In: *CAV*. Vol. 6174. Lecture Notes in Computer Science. 2010. DOI: [10.1007/978-3-642-14295-6\\_24](https://doi.org/10.1007/978-3-642-14295-6_24).
- [51] Anian Ruoss, Mislav Balunovic, Marc Fischer and Martin T. Vechev. ‘Learning Certified Individually Fair Representations’. In: *NeurIPS*. 2020. URL: <https://proceedings.neurips.cc/paper/2020/hash/55d491cf951b1b920900684d71419282-Abstract.html>.



- [52] Gagandeep Singh, Timon Gehr, Markus Püschel and Martin T. Vechev. ‘An Abstract Domain for Certifying Neural Networks’. In: *Proc. ACM Program. Lang.* 3.POPL (2019). DOI: [10.1145/3290354](https://doi.org/10.1145/3290354).
- [53] Christian Szegedy, Wojciech Zaremba, Ilya Sutskever, Joan Bruna, Dumitru Erhan, Ian J. Goodfellow and Rob Fergus. ‘Intriguing properties of neural networks’. In: *ICLR (Poster)*. 2014. DOI: [10.48550/ARXIV.1312.6199](https://doi.org/10.48550/ARXIV.1312.6199).
- [54] Vincent Tjeng, Kai Y. Xiao and Russ Tedrake. ‘Evaluating Robustness of Neural Networks with Mixed Integer Programming’. In: *ICLR (Poster)*. 2019. URL: <https://openreview.net/forum?id=HyGIdiRqtm>.
- [55] Hoang-Dung Tran, Stanley Bak, Weiming Xiang and Taylor T. Johnson. ‘Verification of Deep Convolutional Neural Networks Using ImageStars’. In: *CAV (1)*. Vol. 12224. Lecture Notes in Computer Science. 2020. DOI: [10.1007/978-3-030-53288-8\\_2](https://doi.org/10.1007/978-3-030-53288-8_2).
- [56] Hoang-Dung Tran, Xiaodong Yang, Diego Manzananas Lopez, Patrick Musau, Luan Viet Nguyen, Weiming Xiang, Stanley Bak and Taylor T. Johnson. ‘NNV: The Neural Network Verification Tool for Deep Neural Networks and Learning-Enabled Cyber-Physical Systems’. In: *CAV (1)*. Vol. 12224. Lecture Notes in Computer Science. 2020. DOI: [10.1007/978-3-030-53288-8\\_1](https://doi.org/10.1007/978-3-030-53288-8_1).
- [57] Caterina Urban, Maria Christakis, Valentin Wüstholtz and Fuyuan Zhang. ‘Perfectly parallel fairness certification of neural networks’. In: *Proc. ACM Program. Lang.* 4.OOPSLA (2020). DOI: [10.1145/3428253](https://doi.org/10.1145/3428253).
- [58] Shiqi Wang, Kexin Pei, Justin Whitehouse, Junfeng Yang and Suman Jana. ‘Efficient Formal Safety Analysis of Neural Networks’. In: *NeurIPS*. 2018. URL: <https://proceedings.neurips.cc/paper/2018/hash/2ecd2bd94734e5dd392d8678bc64cdab-Abstract.html>.
- [59] Shiqi Wang, Kexin Pei, Justin Whitehouse, Junfeng Yang and Suman Jana. ‘Formal Security Analysis of Neural Networks using Symbolic Intervals’. In: *USENIX Security Symposium*. 2018. URL: <https://www.usenix.org/conference/usenixsecurity18/presentation/wang-shiqi>.
- [60] Tsui-Wei Weng, Pin-Yu Chen, Lam M. Nguyen, Mark S. Squillante, Akhilan Boopathy, Ivan V. Oseledets and Luca Daniel. ‘PROVEN: Verifying Robustness of Neural Networks with a Probabilistic Approach’. In: *ICML*. Vol. 97. Proceedings of Machine Learning Research. 2019. URL: <http://proceedings.mlr.press/v97/weng19a.html>.
- [61] Tsui-Wei Weng, Huan Zhang, Hongge Chen, Zhao Song, Cho-Jui Hsieh, Luca Daniel, Duane S. Boning and Inderjit S. Dhillon. ‘Towards Fast Computation of Certified Robustness for ReLU Networks’. In: *ICML*. Vol. 80. Proceedings of Machine Learning Research. 2018. URL: <http://proceedings.mlr.press/v80/weng18a.html>.
- [62] Eric Wong and J. Zico Kolter. ‘Provable Defenses against Adversarial Examples via the Convex Outer Adversarial Polytope’. In: *ICML*. Vol. 80. Proceedings of Machine Learning Research. 2018. URL: <http://proceedings.mlr.press/v80/wong18a.html>.
- [63] Haoze Wu, Omri Isac, Aleksandar Zeljić, Teruhiro Tagomori, Matthew Daggitt, Wen Kokke, Idan Refaeli, Guy Amir, Kyle Julian, Shahaf Bassan, Pei Huang, Ori Lahav, Min Wu, Min Zhang, Ekaterina Komendantskaya, Guy Katz and Clark Barrett. ‘Marabou 2.0: A Versatile Formal Analyzer of Neural Networks’. In: *CoRR* abs/2401.14461 (2024). DOI: [10.48550/arXiv.2401.14461](https://doi.org/10.48550/arXiv.2401.14461).
- [64] Kaidi Xu, Zhouxing Shi, Huan Zhang, Yihan Wang, Kai-Wei Chang, Minlie Huang, Bhavya Kailkhura, Xue Lin and Cho-Jui Hsieh. ‘Automatic Perturbation Analysis for Scalable Certified Robustness and Beyond’. In: *NeurIPS*. 2020. URL: <https://proceedings.neurips.cc/paper/2020/hash/0cbc5671ae26f67871cb914d81ef8fc1-Abstract.html>.



- [65] Kaidi Xu, Huan Zhang, Shiqi Wang, Yihan Wang, Suman Jana, Xue Lin and Cho-Jui Hsieh. ‘Fast and Complete: Enabling Complete Neural Network Verification with Rapid and Massively Parallel Incomplete Verifiers’. In: *ICLR*. 2021. URL: <https://openreview.net/forum?id=nVZtXBI6LNn>.
- [66] Huan Zhang, Shiqi Wang, Kaidi Xu, Linyi Li, Bo Li, Suman Jana, Cho-Jui Hsieh and J. Zico Kolter. ‘General Cutting Planes for Bound-Propagation-Based Neural Network Verification’. In: *NeurIPS*. 2022. URL: <https://openreview.net/forum?id=5haAJAcofjc>.
- [67] Huan Zhang, Tsui-Wei Weng, Pin-Yu Chen, Cho-Jui Hsieh and Luca Daniel. ‘Efficient Neural Network Robustness Certification with General Activation Functions’. In: *NeurIPS*. 2018. URL: <https://proceedings.neurips.cc/paper/2018/hash/d04863f100d59b3eb688a11f95b0ae60-Abstract.html>.

## A Probabilistic Verification Problems

This sections contains the formal definitions of all probabilistic verification problems in this paper. First of all, we provide a detailed derivation of Example 1

**Example** (Derivation of Example 1). Let  $\mathcal{X} \subset \mathbb{R}^n$ ,  $A \subset \{1, \dots, n\}$ ,  $a \in A$ ,  $\text{net} : \mathbb{R}^n \rightarrow \mathbb{R}^2$  and  $\gamma$  be as in Example 1. We rewrite Equation (1) as

$$\begin{aligned}
& \frac{\mathbb{P}_{\mathbf{x}}[\text{net}(\mathbf{x}) = \text{yes} \mid \mathbf{x} \text{ is disadvantaged}]}{\mathbb{P}_{\mathbf{x}}[\text{net}(\mathbf{x}) = \text{yes} \mid \mathbf{x} \text{ is advantaged}]} \geq \gamma \\
\iff & \frac{\mathbb{P}_{\mathbf{x}}[\text{net}(\mathbf{x})_1 - \text{net}(\mathbf{x})_2 \geq 0 \mid \mathbf{x}_a \leq 0]}{\mathbb{P}_{\mathbf{x}}[\text{net}(\mathbf{x})_1 - \text{net}(\mathbf{x})_2 \geq 0 \mid \mathbf{x}_a \geq 1]} \geq \gamma \\
\iff & \frac{\mathbb{P}_{\mathbf{x}}[\text{net}(\mathbf{x})_1 - \text{net}(\mathbf{x})_2 \geq 0 \wedge \mathbf{x}_a \leq 0] / \mathbb{P}_{\mathbf{x}}[\mathbf{x}_a \leq 0]}{\mathbb{P}_{\mathbf{x}}[\text{net}(\mathbf{x})_1 - \text{net}(\mathbf{x})_2 \geq 0 \wedge \mathbf{x}_a \geq 1] / \mathbb{P}_{\mathbf{x}}[\mathbf{x}_a \geq 1]} \geq \gamma \\
\iff & \frac{\mathbb{P}_{\mathbf{x}}[\min(\text{net}(\mathbf{x})_1 - \text{net}(\mathbf{x})_2, -\mathbf{x}_a) \geq 0] / \mathbb{P}_{\mathbf{x}}[-\mathbf{x}_a \geq 0]}{\mathbb{P}_{\mathbf{x}}[\min(\text{net}(\mathbf{x})_1 - \text{net}(\mathbf{x})_2, \mathbf{x}_a - 1) \geq 0] / \mathbb{P}_{\mathbf{x}}[\mathbf{x}_a - 1 \geq 0]} \geq \gamma \\
\iff & \frac{\mathbb{P}_{\mathbf{x}}[g_{\text{Sat}}^{(1)}(\mathbf{x}, \text{net}(\mathbf{x})) \geq 0] / \mathbb{P}_{\mathbf{x}}[g_{\text{Sat}}^{(2)}(\mathbf{x}, \text{net}(\mathbf{x})) \geq 0]}{\mathbb{P}_{\mathbf{x}}[g_{\text{Sat}}^{(3)}(\mathbf{x}, \text{net}(\mathbf{x})) \geq 0] / \mathbb{P}_{\mathbf{x}}[g_{\text{Sat}}^{(4)}(\mathbf{x}, \text{net}(\mathbf{x})) \geq 0]} - \gamma \geq 0 \\
\iff & f_{\text{Sat}} \left( \mathbb{P}_{\mathbf{x}} \left[ g_{\text{Sat}}^{(1)}(\mathbf{x}, \text{net}(\mathbf{x})) \geq 0 \right], \dots, \mathbb{P}_{\mathbf{x}} \left[ g_{\text{Sat}}^{(4)}(\mathbf{x}, \text{net}(\mathbf{x})) \geq 0 \right] \right) \geq 0
\end{aligned}$$

where  $f_{\text{Sat}}, g_{\text{Sat}}^{(1)}, g_{\text{Sat}}^{(2)}, g_{\text{Sat}}^{(3)}$ , and  $g_{\text{Sat}}^{(4)}$  are as in Example 1.

### A.1 Parity of Qualified Persons

The following probabilistic verification problem concerns verifying the parity of qualified persons, a variant of demographic parity that only considers the subpopulation of persons qualified for, for example, hiring [3]. Let  $\mathcal{X} \subset \mathbb{R}^n$ ,  $A \subset \{1, \dots, n\}$ ,  $a \in A$ , and  $\text{net} : \mathbb{R}^n \rightarrow \mathbb{R}^2$  be as in Example 1. Additionally, let  $q \in \{1, \dots, n\} \setminus A$  and  $\hat{q} \in \mathbb{R}$ , such that persons with  $\mathbf{x}_q \geq \hat{q}$  are considered to be qualified. In their extended set of experiments, Albarghouthi et al. [3] consider a  $q$  that encodes age and  $\hat{q} = 18$  so that only persons who are at least 18 years old are considered to be qualified. The parity of qualified persons fairness notion is

$$\begin{aligned}
& \frac{\mathbb{P}_{\mathbf{x}}[\text{net}(\mathbf{x}) = \text{yes} \mid \mathbf{x} \text{ is disadvantaged} \wedge \mathbf{x} \text{ is qualified}]}{\mathbb{P}_{\mathbf{x}}[\text{net}(\mathbf{x}) = \text{yes} \mid \mathbf{x} \text{ is advantaged} \wedge \mathbf{x} \text{ is qualified}]} \geq \gamma \\
\iff & \frac{\mathbb{P}_{\mathbf{x}}[\text{net}(\mathbf{x})_1 - \text{net}(\mathbf{x})_2 \geq 0 \mid \mathbf{x}_a \leq 0 \wedge \mathbf{x}_q \geq \hat{q}]}{\mathbb{P}_{\mathbf{x}}[\text{net}(\mathbf{x})_1 - \text{net}(\mathbf{x})_2 \geq 0 \mid \mathbf{x}_a \geq 1 \wedge \mathbf{x}_q \geq \hat{q}]} \geq \gamma \\
\iff & \frac{\mathbb{P}_{\mathbf{x}}[\text{net}(\mathbf{x})_1 - \text{net}(\mathbf{x})_2 \geq 0 \mid \min(-\mathbf{x}_a, \mathbf{x}_q - \hat{q}) \geq 0]}{\mathbb{P}_{\mathbf{x}}[\text{net}(\mathbf{x})_1 - \text{net}(\mathbf{x})_2 \geq 0 \mid \min(\mathbf{x}_a - 1, \mathbf{x}_q - \hat{q}) \geq 0]} \geq \gamma \\
\iff & f_{\text{Sat}} \left( \mathbb{P}_{\mathbf{x}} \left[ g_{\text{Sat}}^{(1)}(\mathbf{x}, \text{net}(\mathbf{x})) \geq 0 \right], \dots, \mathbb{P}_{\mathbf{x}} \left[ g_{\text{Sat}}^{(4)}(\mathbf{x}, \text{net}(\mathbf{x})) \geq 0 \right] \right) \geq 0
\end{aligned}$$

where  $\gamma \in [0, 1]$ ,  $f_{\text{Sat}}(p_1, p_2, p_3, p_4) = (p_1 p_4) / (p_2 p_3) - \gamma$ ,  $g_{\text{Sat}}^{(1)}(\mathbf{x}, \text{net}(\mathbf{x})) = \min(\text{net}(\mathbf{x})_1 - \text{net}(\mathbf{x})_2, -\mathbf{x}_a, \mathbf{x}_q - \hat{q})$ ,  $g_{\text{Sat}}^{(2)}(\mathbf{x}, \text{net}(\mathbf{x})) = \min(-\mathbf{x}_a, \mathbf{x}_q - \hat{q})$ ,  $g_{\text{Sat}}^{(3)}(\mathbf{x}, \text{net}(\mathbf{x})) = \min(\text{net}(\mathbf{x})_1 - \text{net}(\mathbf{x})_2, \mathbf{x}_a - 1, \mathbf{x}_q - \hat{q})$ , and  $g_{\text{Sat}}^{(4)}(\mathbf{x}, \text{net}(\mathbf{x})) = \min(\mathbf{x}_a - 1, \mathbf{x}_q - \hat{q})$ .

### A.2 ACAS Xu Safety

Next, we consider Equation (2) for an ACAS Xu network, where to be safe means satisfying property  $\phi_2$  of Katz et al. [34]. For quantifying the number of violations, we first define what

it means for an ACAS Xu neural network  $\text{net} : \mathbb{R}^5 \rightarrow \mathbb{R}^5$  to violate  $\phi_2$ . Using the satisfaction functions of Bauer-Marquart et al. [9], violating  $\phi_2$  means

$$g_{\text{Sat}}(\mathbf{x}, \text{net}(\mathbf{x})) = \max_{i=1}^5 \text{net}(\mathbf{x})_i - \text{net}(\mathbf{x})_1 < 0 \quad \forall \mathbf{x} \in \mathcal{X}_{\phi_2} \cap \mathcal{X}, \quad (7)$$

where  $\mathcal{X}$  is the bounded hyperrectangular input space of  $\text{net}$  and

$$\mathcal{X}_{\phi_2} = [55947.961, \infty] \times \mathbb{R}^2 \times [1145, \infty] \times [-\infty, 60].$$

We refer to Katz et al. [34] for an interpretation of  $\phi_2$  in the application context. Quantifying the number of violations with respect to  $\phi_2$  corresponds to computing

$$\ell \leq \mathbb{P}_{\mathbf{x}}[g_{\text{Sat}}(\mathbf{x}, \text{net}(\mathbf{x})) < 0] = \mathbb{P}_{\mathbf{x}}[-g_{\text{Sat}}(\mathbf{x}, \text{net}(\mathbf{x})) \geq 0] \leq u,$$

where  $g_{\text{Sat}}$  is as in Equation (7) and  $\mathbf{x}$  is uniformly distributed on  $\mathcal{X}_{\phi_2} \cap \mathcal{X}$  with all points outside  $\mathcal{X}_{\phi_2} \cap \mathcal{X}$  having zero probability.

### A.3 ACAS Xu Robustness

For the ACAS Xu robustness experiment in Section 6.3, we solve five probabilistic verification problems for each reference input  $\mathbf{x}$  – one for each of the five classes. Our goal is to bound the probability of  $\text{net}$  classifying an input  $\mathbf{x}'$  as class  $i \in \{1, \dots, 5\}$ , where  $\mathbf{x}'$  is close to the reference input  $\mathbf{x}$  in the first two dimensions and identical to  $\mathbf{x}$  in the remaining dimensions.

Let  $\text{net}$  be the ACAS Xu network  $N_{1,1}$  of Katz et al. [34] with input space  $\mathcal{X} = [\underline{\mathbf{x}}, \bar{\mathbf{x}}]$ . Let  $\mathbf{x}$  be a reference input. Note that the ACAS Xu networks assign the class with the *minimal* score to an input instead of using the maximal score. For bounding the probability of obtaining class  $i \in \{1, \dots, 5\}$  for inputs close to  $\mathbf{x}$ , we compute bounds on

$$\mathbb{P}_{\mathbf{x}'}[g_{\text{Sat}}(\mathbf{x}', \text{net}(\mathbf{x}')) \geq 0],$$

where  $g_{\text{Sat}}(\mathbf{x}', \text{net}(\mathbf{x}')) = \min_{j=1}^5 \text{net}(\mathbf{x}')_j - \text{net}(\mathbf{x}')_i$  and  $\mathbf{x}'$  is uniformly distributed on the set

$$\mathcal{X} \cap ([\mathbf{x}_{1:2} - 0.05 \cdot \mathbf{w}_{1:2}, \mathbf{x}_{1:2} + 0.05 \cdot \mathbf{w}_{1:2}] \times \{\mathbf{x}_{3:5}\}),$$

where  $\mathbf{w} = \bar{\mathbf{x}} - \underline{\mathbf{x}}$  and  $\mathbf{z}_{i:j}$  is the vector containing the elements  $i, \dots, j$  of a vector  $\mathbf{z}$ .

## B Interval Arithmetic

This section introduces additional interval arithmetic bounding rules for linear functions, multiplication, and division, complementing the interval arithmetic bounding rules for monotone functions in Section 3.2.1. Furthermore, we provide Theorems 5.1 and 6.1 of Moore et al. [42] for reference.

### B.1 Bounding Rules

Let  $f^{(k)}$  be as in Section 3.2.1. First, consider the multiplication of two scalars, that is,  $f^{(k)}(z, w) = zw$  where  $\underline{z} \leq z \leq \bar{z}$  and  $\underline{w} \leq w \leq \bar{w}$ . We have

$$\min(\underline{z}\underline{w}, \underline{z}\bar{w}, \bar{z}\underline{w}, \bar{z}\bar{w}) \leq z_1 z_2 \leq \max(\underline{z}\underline{w}, \underline{z}\bar{w}, \bar{z}\underline{w}, \bar{z}\bar{w}).$$

For the element-wise multiplication of vectors, we apply the above rule to each element separately. Multiplication of several arguments can be rewritten as several multiplications of two arguments.

Now, consider computing bounds of the reciprocal  $f^{(k)}(z) = \frac{1}{z}$  with  $\underline{z} \leq z \leq \bar{z}$ . We differentiate the following cases

$$\begin{aligned} \frac{1}{\bar{z}} \leq \frac{1}{z} & \quad \text{if } 0 \notin (\underline{z}, \bar{z}] & \quad \frac{1}{z} \leq \frac{1}{\underline{z}} & \quad \text{if } 0 \notin [z, \bar{z}) \\ -\infty \leq \frac{1}{z} & \quad \text{if } 0 \in (\underline{z}, \bar{z}] & \quad \frac{1}{z} \leq \infty & \quad \text{if } 0 \in [z, \bar{z}). \end{aligned}$$

Using bounds on the reciprocal, we can compute bounds on a division by rewriting division as multiplication by the reciprocal. Lastly, for a linear function  $f^{(k)}(\mathbf{z}) = \mathbf{A}\mathbf{z} + \mathbf{b}$  where  $\underline{\mathbf{z}} \leq \mathbf{z} \leq \bar{\mathbf{z}}$ , we have

$$\mathbf{A}^+ \underline{\mathbf{z}} + \mathbf{A}^- \bar{\mathbf{z}} + \mathbf{b} \leq \mathbf{A}\mathbf{z} + \mathbf{b} \leq \mathbf{A}^+ \bar{\mathbf{z}} + \mathbf{A}^- \underline{\mathbf{z}} + \mathbf{b},$$

where  $\mathbf{A}_{i,j}^+ = \max(0, \mathbf{A}_{i,j})$  and  $\mathbf{A}_{i,j}^- = \min(0, \mathbf{A}_{i,j})$ .

## B.2 Selected Theorems of Moore et al. [42]

We include Theorems 5.1 and 6.1 of Moore et al. [42] and relevant definitions for reference. Let  $\mathbb{H}^n = \{[\underline{\mathbf{x}}, \bar{\mathbf{x}}] \mid \underline{\mathbf{x}}, \bar{\mathbf{x}} \in \mathbb{R}^n, \underline{\mathbf{x}} \leq \bar{\mathbf{x}}\}$  be the set of hyperrectangles in  $\mathbb{R}^n$ . Let  $w : 2^{\mathbb{R}^n} \rightarrow \mathbb{R}_{\geq 0}$  with

$$w(\mathcal{X}') = \max_{i \in \{1, \dots, n\}} (\max_{\mathbf{x} \in \mathcal{X}'} \mathbf{x}_i - \min_{\mathbf{x} \in \mathcal{X}'} \mathbf{x}_i)$$

be the *width* of a set. We denote the *image* of a hyperrectangle  $[\underline{\mathbf{x}}, \bar{\mathbf{x}}]$  under  $f : \mathbb{R}^n \rightarrow \mathbb{R}^m$  as  $f([\underline{\mathbf{x}}, \bar{\mathbf{x}}]) = \{f(\mathbf{x}) \mid \mathbf{x} \in [\underline{\mathbf{x}}, \bar{\mathbf{x}}]\}$ .

### B.2.1 Definitions

Theorem 5.1 of Moore et al. [42] applies to inclusion isotonic interval extensions as defined below.

**Definition 3.** Let  $F : \mathbb{H}^n \rightarrow \mathbb{H}^m$  and  $f : \mathbb{R}^n \rightarrow \mathbb{R}^m$ .

- $F$  is an *interval extensions* of  $f$  if  $\forall \mathbf{x} \in \mathbb{R}^n : F([\mathbf{x}, \mathbf{x}]) = [f(\mathbf{x}), f(\mathbf{x})]$ .
- $F$  is *inclusion isotonic* if  $\forall [\underline{\mathbf{x}}, \bar{\mathbf{x}}], [\underline{\mathbf{x}}', \bar{\mathbf{x}}'] \in \mathbb{H}^n, [\underline{\mathbf{x}}', \bar{\mathbf{x}}'] \subseteq [\underline{\mathbf{x}}, \bar{\mathbf{x}}] : F([\underline{\mathbf{x}}', \bar{\mathbf{x}}']) \subseteq F([\underline{\mathbf{x}}, \bar{\mathbf{x}}])$ .

Theorem 6.1 of Moore et al. [42] requires an inclusion isotonic *Lipschitz* interval extension.

**Definition 4.** Let  $F : \mathbb{H}^n \rightarrow \mathbb{H}^m$  be an interval extension of  $f : \mathbb{R}^n \rightarrow \mathbb{R}^m$ .  $F$  is *Lipschitz* if there exists an  $L \in \mathbb{R}$  such that  $\forall [\underline{\mathbf{x}}, \bar{\mathbf{x}}] \in \mathbb{H}^n : w(F([\underline{\mathbf{x}}, \bar{\mathbf{x}}])) \leq Lw([\underline{\mathbf{x}}, \bar{\mathbf{x}}])$ .

Interval arithmetic, as introduced in Section 3.2.1, corresponds to *natural interval extensions* in Moore et al. [42]. As Moore et al. [42] show, natural interval extensions – and, therefore, interval arithmetic as introduced in Section 3.2.1 – satisfy Definitions 3 and 4.

### B.2.2 Theorems

Theorem 5.1 of Moore et al. [42] is known as the fundamental theorem of interval analysis. Theorem 6.1 of Moore et al. [42] underlines our completeness proof in Section 5.2.

**Theorem** (Theorem 5.1 of Moore et al. [42]). *If  $F : \mathbb{H}^n \rightarrow \mathbb{H}^m$  is an inclusion isotonic interval extension of  $f : \mathbb{R}^n \rightarrow \mathbb{R}^m$ , we have  $f([\underline{\mathbf{x}}, \bar{\mathbf{x}}]) \subseteq F([\underline{\mathbf{x}}, \bar{\mathbf{x}}])$  for every  $[\underline{\mathbf{x}}, \bar{\mathbf{x}}] \in \mathbb{H}^n$ .*

**Theorem** (Theorem 6.1 of Moore et al. [42]). *Let  $F : \mathbb{H}^n \rightarrow \mathbb{H}^m$  be an inclusion isotonic Lipschitz interval extension of  $f : \mathbb{R}^n \rightarrow \mathbb{R}^m$ . Let  $\mathcal{X} = [\underline{\mathbf{x}}, \bar{\mathbf{x}}] \in \mathbb{H}^n$ . We define the  $M$ -step uniform subdivision of  $[\underline{\mathbf{x}}, \bar{\mathbf{x}}]$  with  $M \in \mathbb{N}$  as*

$$\mathcal{X}_{i,j} = \left[ \underline{\mathbf{x}}_i + (j-1) \frac{w([\underline{\mathbf{x}}_i, \bar{\mathbf{x}}_i])}{M}, \underline{\mathbf{x}}_i + j \frac{w([\underline{\mathbf{x}}_i, \bar{\mathbf{x}}_i])}{M} \right], \quad j \in \{1, \dots, M\}.$$

Further, let

$$F^{(M)}([\underline{\mathbf{x}}, \bar{\mathbf{x}}]) = \bigcup_{j_i=1}^M F(\mathcal{X}_{1,j_1} \times \dots \times \mathcal{X}_{n,j_n}).$$

It holds that

$$w(F^{(M)}([\underline{\mathbf{x}}, \bar{\mathbf{x}}])) - w(f([\underline{\mathbf{x}}, \bar{\mathbf{x}}])) \leq 2L \frac{w(\mathcal{X})}{M},$$

where  $L$  is the Lipschitz constant of  $F$ .

In this paper, we apply Theorem 6.1 to a refinement of the input space finer than some uniform subdivision, meaning that every part of the input space refinement is contained in a part of the uniform subdivision. Theorem 6.1 extends to such refinements of the input space since interval arithmetic is inclusion isotonic.

## C Experiments

This section contains additional details on the experiments from Section 6 and additional experimental results.

### C.1 Hardware

We run all our experiments in Section 6 and this section on a workstation running Ubuntu 22.04 with an Intel i7-4820K CPU, 32 GB of memory and no GPU (HW1). This CPU model is ten years old (introduced in late 2013) and has four cores and eight threads. Converse et al. [19] use an AMD EPYC 7401P CPU for their ACAS Xu robustness experiments, limiting their tool to use 46 threads and at most 4GB of memory. AMD EPYC 7401P was introduced in mid-2017, targeting servers. Marzari et al. [40] use a Ubuntu 22.04 workstation with an Intel i5-13600KF CPU and an Nvidia GeForce RTX 4070 Ti GPU. This CPU was introduced in end-2022 and has 14 cores with 20 threads. Figure 3 contains the CPU comparison from [versus.com](https://www.versus.com). As the figure shows, our HW1 is less performant when considering both the theoretical performance according to the hardware specification and the actual performance on a series of computational benchmarks. Therefore, HW1 is inferior in computation power to the hardware used by Converse et al. [19] and Marzari et al. [40]. Additional experiments on recent hardware are contained in Appendix D.

### C.2 FairSquare Benchmark

We provide additional details on the FairSquare benchmark and present additional results.

#### C.2.1 Extended Description of the Benchmark

The input space in the FairSquare benchmark consists of three continuous variables for the age, the years of education ('edu'), and the yearly gain in capital of a person ('capital gain'), respectively, as well as an additional discrete protected variable indicating a person's (assumed binary) sex. The neural networks use 'age' and 'edu' or 'age', 'edu' and 'capital gain', depending on the network architecture, to predict whether a person has a high salary (higher than \$50 000). The three input distributions used by the FairSquare benchmark are



(a) HW1 ■ vs. Converse et al. [19] ■

(b) HW1 ■ vs. Marzari et al. [40] ■

Figure 3: **Hardware Comparison from versus.com.** The figures are taken from <https://versus.com/en/amd-epyc-7401p-vs-intel-core-i7-6700> and <https://versus.com/en/intel-core-i5-13600kf-vs-intel-core-i7-4820k>, respectively. Printouts of both web pages are available in the supplementary material.

1. the combination of three independent normal distributions for the continuous variables and a Bernoulli distribution for the person’s sex,
2. a Bayesian Network with the structure in Figure 4 introducing correlations between the variables that are similarly distributed as for the independent input distribution (‘Bayes Net 1’), and
3. the same Bayesian Network augmented with a constraint that the years of education may not exceed a person’s age (‘Bayes Net 2’).

The integrity constraint is implemented by Albarghouthi et al. [3] as a post-processing of the samples from the Bayesian Network. In particular, an person’s years of education are set to the person’s age if the sampled years of education are larger than the sampled age. We introduce a pre-processing layer before the neural network we want to verify to implement this integrity constraint in our setting. This pre-processing layer computes  $edu' = \min(edu, age)$  and leaves the remaining inputs unchanged.

Besides experiments on the demographic parity fairness notion, the extended FairSquare benchmarks also include experiments on the parity of qualified persons fairness notion as defined in Appendix A.1. For both fairness notions, the FairSquare benchmark uses a fairness threshold of  $\gamma = 0.85$ .

### C.2.2 Extended Results

Table 4 contains the comparison of PV and FairSquare on the extended set of FairSquare benchmarks from Albarghouthi et al. [3]. The extended set of benchmarks also contains one instance which PV can not solve within the time budget. In this instance, the bounds computed up to the timeout indicate that the probability ratio on which we compute bounds (see Equation (1)) is close to the



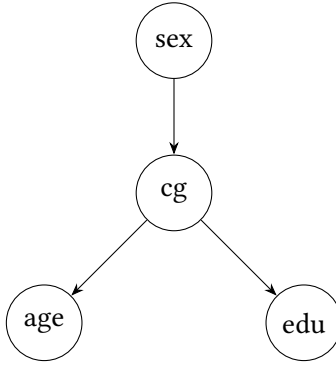


Figure 4: **FairSquare Bayes Net 1.** The network structure of the Bayesian Network from the FairSquare benchmark. In this figure, ‘cg’ denotes the capital gain variable and ‘edu’ denotes the number of years of education.

threshold of 0.85 above which the probability ratio should lie according to the fairness notion. Relating this to Theorem 2, the above might mean that the neural network is not strictly feasible or infeasible for the probabilistic verification problem, at least not by a large margin. This shows that the scalability of PV not only depends on the input size and the network complexity but also on additional factors, such as the margin with which a neural network is feasible or infeasible for the probabilistic verification problem.

As Table 4 shows, there are also two benchmark instances in which FairSquare is substantially faster than PV. However, these are outliers in the entire set of benchmarks. Additionally, they disappear when considering input distributions that were clipped to realistic ranges for the inputs (for example, no negative values of age). Table 5 contains the results of running PV on these *clipped* input distributions. Using realistic input distributions accelerates PV, except for three benchmark instances. It also reveals that some FairSquare networks are, in fact, unfair under realistic conditions. Faithfully comparing these results with FairSquare is not feasible since FairSquare does not implement truncated normal distributions, which we use for the clipped input distributions.

### C.3 ACAS Xu Safety

We provide a comparison of ProbabilityBounds with  $\varepsilon$ -ProVe [39] on all 36 ACAS Xu networks to which property  $\phi_2$  applies [34]. These results are contained in Table 6, revealing that the networks in Table 3 are outliers. However, ProbabilityBounds still computes tighter sound bounds faster than  $\varepsilon$ -ProVe computes probably sound bounds for 13 of the 36 networks.

Table 7 contains additional results for running ProbabilityBounds with a finer grid of time budgets on the networks from Table 3 and two additional challenging instances from Katz et al. [34].

### C.4 ACAS Xu Robustness

Table 8 contains the bounds computed by ProbabilityBounds for each reference input and each output class: COC (Clear-of-Conflict), WL (steer Weak Left), WR (steer Weak Right), SL (steer Strong Left), and SR (steer Strong Right). The table reveals that the ACAS Xu network  $N_{1,1}$  tends to classify inputs as Clear-of-Conflict (COC), regardless of the class assigned to the reference input. This insight does not agree with the insight drawn by Converse et al. [19]. However, both results are based on a tiny sample of the input space of only 25 points. Obtaining valid results requires considering a significantly larger sample of the input space or quantifying global robustness [33].

Benchmark Instance		Demographic Parity			Parity of Qualified Persons		
		Runtime (s)			Runtime (s)		
net	$\mathbb{P}_x$	PV	FairSquare	Fair?	PV	FairSquare	Fair?
NN <sub>2,1</sub>	independent	<b>1.3</b>	2.1	✓	<b>1.2</b>	3.2	✓
NN <sub>2,1</sub>	Bayes Net 1	<b>2.2</b>	75.5	✓	<b>3.2</b>	37.8	✓
NN <sub>2,1</sub>	Bayes Net 2	<b>3.6</b>	50.5	✓	<b>6.1</b>	25.5	✓
NN <sub>2,2</sub>	independent	<b>1.8</b>	4.2	✓	<b>1.7</b>	6.8	✓
NN <sub>2,2</sub>	Bayes Net 1	<b>3.3</b>	33.3	✓	622.2	<b>60.4</b>	✓
NN <sub>2,2</sub>	Bayes Net 2	<b>4.9</b>	58.6	✓	782.8	<b>60.7</b>	✓
NN <sub>3,2</sub>	independent	<b>2.2</b>	450.5	✓	<b>2.0</b>	657.0	✓
NN <sub>3,2</sub>	Bayes Net 1	<b>4.4</b>	TO	✓	TO	TO	?
NN <sub>3,2</sub>	Bayes Net 2	<b>6.9</b>	TO	✓	<b>11.5</b>	TO	✓

Table 4: **FairSquare Benchmark**. The first two columns indicate the neural network net that is verified and the input probability distribution  $\mathbb{P}_x$ , respectively. We verify two fairness notions: demographic parity and parity of qualified persons. For each fairness notion, the first two columns contain the runtime of PV and FairSquare in seconds. Here, ‘TO’ indices timeout (900s). The last column contains the result of the verification with PV. The results in this table are for the non-clipped input distributions that include unrealistic values, such as negative values of a person’s age.

Benchmark Instance		Demographic Parity		Parity of Qualified Persons	
		PV		PV	
net	$\mathbb{P}_x$	Runtime	Fair?	Runtime	Fair?
NN <sub>2,1</sub>	independent clipped	1.1	✓	1.1	✓
NN <sub>2,1</sub>	Bayes Net 1 clipped	1.8	✓	2.6	✓
NN <sub>2,1</sub>	Bayes Net 2 clipped	2.9	✓	5.4	✓
NN <sub>2,2</sub>	independent clipped	1.7	✓	1.6	✓
NN <sub>2,2</sub>	Bayes Net 1 clipped	2.8	✓	3.8	✓
NN <sub>2,2</sub>	Bayes Net 2 clipped	4.3	✓	7.5	✓
NN <sub>3,2</sub>	independent clipped	1.3	✓	1.3	✓
NN <sub>3,2</sub>	Bayes Net 1 clipped	5.0	✗	6.2	✗
NN <sub>3,2</sub>	Bayes Net 2 clipped	7.8	✗	TO	?

Table 5: **FairSquare Benchmark for Realistic Input Distributions**. This table contains the results for running PV on the FairSquare benchmarks with clipped input distributions that rule out unrealistic values, such as negative values of a person’s age. The first two columns indicate the neural network net that is verified and the input probability distribution  $\mathbb{P}_x$ , respectively. The following columns contain the runtime of PV in seconds and the verification result for the demographic parity and the parity of qualified persons fairness notions. A runtime of ‘TO’ indices timeout (900s).

$\phi$	net	ProbabilityBounds			$\varepsilon$ -ProVe	
		10s	30s	60s	99.9% confid.	
		$\ell, u$	$\ell, u$	$\ell, u$	$u$	Rt
$\phi_2$	$N_{2,1}$	0.04%, 3.14%	0.08%, 2.48% ←	0.16%, 2.05%	2.58%	64.00s
	$N_{2,2}$	0.00%, 3.55%	0.11%, 2.92%	0.24%, 2.67%	2.49% ←	43.60s
	$N_{2,3}$	0.54%, 3.43% ←	0.89%, 3.05%	1.01%, 2.69%	3.58%	54.50s
	$N_{2,4}$	0.00%, 2.74% ←	0.03%, 2.30%	0.05%, 2.08%	2.78%	65.90s
	$N_{2,5}$	0.05%, 4.16%	0.19%, 3.70%	0.41%, 3.22%	3.06% ←	47.20s
	$N_{2,6}$	0.02%, 3.71%	0.20%, 3.09%	0.33%, 2.58%	2.32% ←	45.40s
	$N_{2,7}$	0.42%, 5.54%	1.02%, 5.03%	1.32%, 4.42%	4.04% ←	47.40s
	$N_{2,8}$	0.98%, 3.80%	1.25%, 3.04% ←	1.38%, 2.79%	3.28%	52.90s
	$N_{2,9}$	0.02%, 2.90%	0.09%, 1.67%	0.11%, 1.41%	0.58% ←	10.80s
$N_{3,1}$	$N_{3,1}$	0.26%, 4.26%	0.55%, 3.33%	0.88%, 2.78% ←	2.84%	40.30s
	$N_{3,2}$	0.00%, 3.45%	0.00%, 1.58%	0.00%, 1.16%	0.00% ←	1.00s
	$N_{3,3}$	0.00%, 3.06%	0.00%, 1.84%	0.00%, 0.87%	0.00% ←	1.00s
	$N_{3,4}$	0.00%, 3.24%	0.07%, 1.96%	0.13%, 1.52%	1.36% ←	30.80s
	$N_{3,5}$	0.37%, 2.83%	0.54%, 2.30% ←	0.66%, 2.12%	2.67%	41.90s
	$N_{3,6}$	0.00%, 6.73%	0.00%, 5.50%	0.03%, 5.26%	2.69% ←	31.60s
	$N_{3,7}$	0.00%, 5.77%	0.00%, 4.61%	0.00%, 3.66%	0.91% ←	30.10s
	$N_{3,8}$	0.17%, 5.48%	0.27%, 4.68%	0.34%, 3.76%	2.79% ←	61.40s
	$N_{3,9}$	0.34%, 4.77%	1.07%, 4.02%	1.42%, 3.73%	3.52% ←	32.10s
$N_{4,1}$	$N_{4,1}$	0.00%, 2.89%	0.02%, 1.95%	0.05%, 1.57%	1.16% ←	26.40s
	$N_{4,2}$	0.00%, 2.55%	0.00%, 1.65%	0.00%, 1.33%	0.00% ←	1.00s
	$N_{4,3}$	0.19%, 2.90%	0.37%, 2.66%	0.62%, 2.28% ←	2.43%	40.80s
	$N_{4,4}$	0.05%, 2.42%	0.18%, 2.23%	0.28%, 2.00%	1.94% ←	40.00s
	$N_{4,5}$	0.04%, 4.66%	0.23%, 3.58%	0.64%, 3.02%	2.85% ←	40.70s
	$N_{4,6}$	0.39%, 4.45%	0.97%, 3.52%	1.22%, 3.28%	3.22% ←	38.80s
	$N_{4,7}$	0.18%, 4.28%	0.39%, 3.42%	0.63%, 3.02%	2.58% ←	29.60s
	$N_{4,8}$	0.20%, 3.89%	0.53%, 3.27% ←	0.88%, 2.82%	3.51%	52.40s
	$N_{4,9}$	0.00%, 3.39%	0.00%, 2.08%	0.01%, 1.65%	0.39% ←	11.00s
$N_{5,1}$	$N_{5,1}$	0.03%, 2.57%	0.32%, 2.13% ←	0.44%, 2.00%	2.14%	34.80s
	$N_{5,2}$	0.24%, 2.71% ←	0.49%, 2.06%	0.53%, 1.95%	3.22%	66.80s
	$N_{5,3}$	0.00%, 1.74%	0.00%, 0.73%	0.00%, 0.53%	0.00% ←	1.00s
	$N_{5,4}$	0.01%, 2.95%	0.15%, 2.35%	0.24%, 2.09% ←	2.31%	54.20s
	$N_{5,5}$	0.77%, 3.37%	1.33%, 2.68% ←	1.38%, 2.63%	2.77%	32.90s
	$N_{5,6}$	0.34%, 4.89%	0.87%, 3.36% ←	1.05%, 3.07%	4.82%	73.50s
	$N_{5,7}$	1.29%, 4.62%	1.82%, 4.12% ←	2.00%, 3.75%	4.27%	44.60s
	$N_{5,8}$	0.95%, 4.12%	1.37%, 3.33% ←	1.58%, 3.11%	3.38%	42.40s
	$N_{5,9}$	0.78%, 3.74%	1.28%, 3.06% ←	1.46%, 2.91%	3.06%	35.60s
	# ←	3	10	3	20	

Table 6: **Comparison of ProbabilityBounds and  $\varepsilon$ -ProVe for ACAS Xu Safety.** A ProbabilityBounds column is marked with an arrow (←) if ProbabilityBounds computes a tighter upper bound than  $\varepsilon$ -ProVe within a certain time budget. If this is not the case for any time budget, the  $\varepsilon$ -ProVe entry is marked with an arrow (←). In total, ProbabilityBounds computes tighter upper bounds within 60s in 16 cases. In 13 cases, it even computes a tighter bound faster than  $\varepsilon$ -ProVe.

		Timeout					
		10s		30s		1m	
$\phi$	net	$\ell, u$	$u - \ell$	$\ell, u$	$u - \ell$	$\ell, u$	$u - \ell$
$\phi_2$	$N_{4,3}$	0.19%, 2.90%	2.71%	0.37%, 2.66%	2.29%	0.62%, 2.28%	1.66%
	$N_{4,9}$	0.00%, 3.39%	3.39%	0.00%, 2.08%	2.08%	0.01%, 1.65%	1.64%
	$N_{5,8}$	0.95%, 4.12%	3.17%	1.37%, 3.33%	1.97%	1.58%, 3.11%	1.53%
$\phi_7$	$N_{1,9}$	0.00%, 94.83%	94.83%	0.00%, 86.28%	86.28%	0.00%, 77.96%	77.96%
$\phi_8$	$N_{2,9}$	0.00%, 70.06%	70.06%	0.00%, 59.38%	59.38%	0.00%, 53.51%	53.51%
		10m		1h			
$\phi$	net	$\ell, u$	$u - \ell$	$\ell, u$	$u - \ell$		
$\phi_2$	$N_{4,3}$	0.97%, 1.97%	1.01%	1.12%, 1.75%	0.63%		
	$N_{4,9}$	0.04%, 0.55%	0.51%	0.08%, 0.30%	0.22%		
	$N_{5,8}$	1.91%, 2.66%	0.76%	1.97%, 2.57%	0.60%		
$\phi_7$	$N_{1,9}$	0.00%, 44.48%	44.48%	0.00%, 27.66%	27.66%		
$\phi_8$	$N_{2,9}$	0.00%, 31.57%	31.57%	0.00%, 14.73%	14.73%		

Table 7: **Extended Probability Bounds Results for ACAS Xu Safety.**

## C.5 MiniACSIncome

We provide additional details on the MiniACSIncome benchmark, including how we construct the dataset and train the networks.

### C.5.1 Dataset

The MiniACSIncome benchmarks are built by sampling about 100 000 entries from the ACS PUMPS 1-Year horizon data for all states of the USA for the year 2018 using the folktables Python package [20]. In line with ACSIncome [20], we only sample individuals older than 16 years, with a yearly income of at least \$100, reported working hours per week of at least 1, and a ‘PWGTP’ (more details in Ding et al. [20]) of at least 1. In total, our dataset contains 102 621 samples.

**Variable Order.** For obtaining the benchmark MiniACSIncome- $i$ ,  $i \in \{1, \dots, 8\}$ , we select  $i$  input variables in the following order: ‘SEX’, ‘COW’, ‘SCHL’, ‘WKHP’, ‘MAR’, ‘RAC1P’, ‘RELP’, ‘AGEP’. We choose ‘SEX’ as the first variable so that we can verify the fairness with respect to ‘SEX’ on every benchmark instance. The order of the remaining variables is chosen based on each variable’s expected predictive value and the number of discrete values. In particular, we select ‘COW’ (class of work), ‘SCHL’ (level of education), and ‘WKHP’ (work hours per week) first, as we consider these variables to be more predictive than ‘MAR’ (marital status), ‘RAC1P’ (races of a person), ‘RELP’ (relationship), and ‘AGEP’ (age of a person). The variables are ordered by their number of discrete values within these groups of expected predictive value. For example, ‘COW’ has nine categories, while ‘WKHP’ has 99 possible integer values.

Table 9 contains the number of input dimensions and the total number of discrete values in each MiniACSIncome- $i$  input space. The input space contains more dimensions than input variables due to the one-hot encoding of all categorical variables.

### C.5.2 Input Distribution

The Bayesian Network input distribution of MiniACSIncome has the network structure depicted in Figure 5. For using ‘AGEP’ as a parent node, we summarised the age groups 17–34, 35–59, and

Reference Input		Target Label											
Label	Input #	COC		WL		WR		SL		SR			
		$\ell, u$	Rt	$\ell, u$	Rt	$\ell, u$	Rt	$\ell, u$	Rt	$\ell, u$	Rt		
COC	1	100%, 100%	0.3	0.0%, 0.0%	0.3	0.0%, 0.0%	0.3	0.0%, 0.0%	0.3	0.0%, 0.0%	0.3	0.0%, 0.0%	0.3
COC	2	99.9%, 100%	0.6	0.0%, 0.0%	0.5	0.0%, 0.1%	0.5	0.0%, 0.0%	0.5	0.0%, 0.0%	0.5	0.0%, 0.0%	0.5
COC	3	91.7%, 91.8%	2.9	1.3%, 1.4%	5.4	1.9%, 2.0%	3.9	2.1%, 2.2%	10.1	2.8%, 2.8%	3.4	2.8%, 2.8%	3.4
COC	4	100%, 100%	0.2	0.0%, 0.0%	0.2	0.0%, 0.0%	0.2	0.0%, 0.0%	0.2	0.0%, 0.0%	0.2	0.0%, 0.0%	0.2
COC	5	100%, 100%	0.4	0.0%, 0.0%	0.4	0.0%, 0.0%	0.4	0.0%, 0.0%	0.4	0.0%, 0.0%	0.4	0.0%, 0.0%	0.4
WL	1	89.9%, 90.0%	1.6	1.6%, 1.7%	30.8	4.7%, 4.8%	1.8	3.6%, 3.7%	31.8	0.0%, 0.0%	1.4	0.0%, 0.0%	1.4
WL	2	92.9%, 93.0%	2.9	2.4%, 2.4%	2.0	3.0%, 3.0%	2.7	1.4%, 1.5%	2.5	0.2%, 0.3%	1.4	0.2%, 0.3%	1.4
WL	3	90.4%, 90.5%	2.9	1.1%, 1.2%	7.5	3.6%, 3.7%	3.3	3.8%, 3.9%	9.1	0.8%, 0.9%	2.1	0.8%, 0.9%	2.1
WL	4	83.6%, 83.7%	16.5	5.4%, 5.5%	44.2	2.6%, 2.7%	41.1	4.6%, 4.7%	49.3	3.5%, 3.6%	51.2	3.5%, 3.6%	51.2
WL	5	96.8%, 96.9%	1.5	2.9%, 3.0%	1.4	0.0%, 0.1%	1.0	0.0%, 0.0%	0.8	0.1%, 0.2%	1.0	0.1%, 0.2%	1.0
WR	1	62.2%, 62.3%	15.2	0.0%, 0.0%	1.1	3.4%, 3.5%	16.1	15.8%, 15.9%	7.3	18.5%, 18.6%	9.9	18.5%, 18.6%	9.9
WR	2	96.6%, 96.7%	1.3	1.5%, 1.6%	1.3	1.7%, 1.8%	1.5	0.0%, 0.1%	1.3	0.0%, 0.1%	1.0	0.0%, 0.1%	1.0
WR	3	94.8%, 94.9%	3.1	0.0%, 0.1%	24.1	1.9%, 2.0%	173.4	0.0%, 0.1%	4.7	3.2%, 3.3%	92.9	3.2%, 3.3%	92.9
WR	4	94.3%, 94.4%	1.8	1.8%, 1.9%	2.2	3.4%, 3.5%	1.9	0.3%, 0.4%	2.0	0.0%, 0.1%	1.2	0.0%, 0.1%	1.2
WR	5	91.1%, 91.2%	3.8	0.8%, 0.9%	6.3	4.2%, 4.3%	7.5	3.0%, 3.1%	10.0	0.7%, 0.8%	4.1	0.7%, 0.8%	4.1
SL	1	81.1%, 81.2%	20.2	2.3%, 2.4%	60.1	4.8%, 4.9%	117.9	4.8%, 4.9%	58.3	6.7%, 6.8%	118.5	6.7%, 6.8%	118.5
SL	2	93.9%, 93.9%	2.7	1.1%, 1.2%	21.2	3.7%, 3.8%	31.3	0.7%, 0.7%	9.2	0.5%, 0.6%	12.4	0.5%, 0.6%	12.4
SL	3	83.3%, 83.4%	9.1	2.8%, 2.9%	13.7	6.5%, 6.6%	33.5	2.1%, 2.2%	12.7	5.0%, 5.1%	27.9	5.0%, 5.1%	27.9
SL	4	81.8%, 81.9%	18.0	3.3%, 3.4%	80.0	5.2%, 5.3%	99.0	5.6%, 5.7%	77.5	4.0%, 4.1%	58.8	4.0%, 4.1%	58.8
SL	5	84.9%, 85.0%	13.3	1.7%, 1.8%	22.4	5.4%, 5.5%	35.5	3.0%, 3.1%	23.7	4.8%, 4.9%	34.3	4.8%, 4.9%	34.3
SR	1	91.0%, 91.1%	4.9	0.0%, 0.1%	2.6	5.2%, 5.3%	50.8	0.0%, 0.1%	2.2	3.6%, 3.7%	28.5	3.6%, 3.7%	28.5
SR	2	87.0%, 87.1%	7.3	0.9%, 1.0%	5.0	5.7%, 5.8%	56.4	1.2%, 1.3%	6.1	5.0%, 5.1%	72.3	5.0%, 5.1%	72.3
SR	3	88.4%, 88.5%	2.7	2.5%, 2.6%	8.1	4.7%, 4.8%	7.3	2.6%, 2.7%	12.1	1.5%, 1.6%	7.4	1.5%, 1.6%	7.4
SR	4	93.0%, 93.1%	5.4	0.7%, 0.8%	47.6	3.7%, 3.8%	86.9	1.0%, 1.1%	25.5	1.4%, 1.5%	29.6	1.4%, 1.5%	29.6
SR	5	79.3%, 79.4%	5.2	0.2%, 0.3%	1.7	9.1%, 9.2%	8.3	3.7%, 3.8%	4.2	7.4%, 7.5%	5.1	7.4%, 7.5%	5.1

Table 8: **ACAS Xu Robustness**. We report the lower and upper bounds ( $\ell, u$ ) ProbabilityBounds computes for the probability that a perturbed input is classified as the target label and the runtime in seconds (Rt) of ProbabilityBounds for computing these bounds. For each combination of unperturbed label, input, and target label, we run ProbabilityBounds until the difference between the lower and the upper bound is at most 0.1%.

	#Input Variables							
	1	2	3	4	5	6	7	8
#Input Dimensions	2	10	34	35	40	49	67	68
#Discrete Values	2	16	382	38K	190K	1.7M	31M	2B
PV Runtime	15.6s	43.1s	125.5s	226.6s	370.6s	690.5s	1329.4s	TO
10-Neuron Network Fair?	×	×	×	×	×	×	×	?

Table 9: MiniACSIncome Details and PV Verification Results.

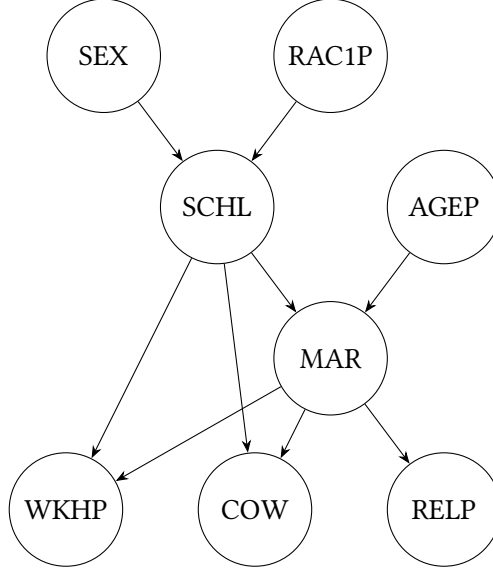


Figure 5: MiniACSIncome Bayesian Network Structure.

60–95. This means that the conditional probability table of ‘MAR’ does not have 78 entries for ‘AGEP’, but three, corresponding to the ranges 17–34, 35–59, and 60–95.

To fit the Bayesian Network, we walk the network from sources to sinks and fit each conditional distribution to match the empirical distribution of the data subset that matches the current condition. For example, for fitting the conditional distribution of ‘SCHL’ given ‘SEX=1’, ‘RAC1P=1’, we select the samples in the dataset having ‘SEX=1’ and ‘RAC1P=1’ and fit the conditional distribution of ‘SCHL’ to match the empirical distribution of these samples. We use categorical distributions for all categorical variables and ‘WKHP’. For ‘AGEP’, we fit a mixture model of four truncated normal distributions that we discretise to integer values.

Figure 6 depict the marginal distributions of 10 000 samples from the fitted Bayesian Network and the empirical marginal distributions of the MiniACSIncome-8 dataset. Figure 7 contains the correlation matrix of the same sample compared to the correlation matrix of MiniACSIncome-8. The Bayesian Network approximates the empirical marginal distribution and the correlation structure of MiniACSIncome-8 reasonably well.

Note that for real-world fairness verification, the input distribution should not be fitted to the same dataset on which the neural network to verify is trained on. Instead, the input distribution needs to be carefully constructed by domain experts. For fairness audits, the input distribution could also be designed adversarially by a fairness auditing entity.

### C.5.3 Training

All MiniACSIncome neural networks are trained on a 56%/14%/30% split of the MiniACSIncome-*i* dataset into training, validation, and testing data. This split is identical for all MiniACSIncome-*i*



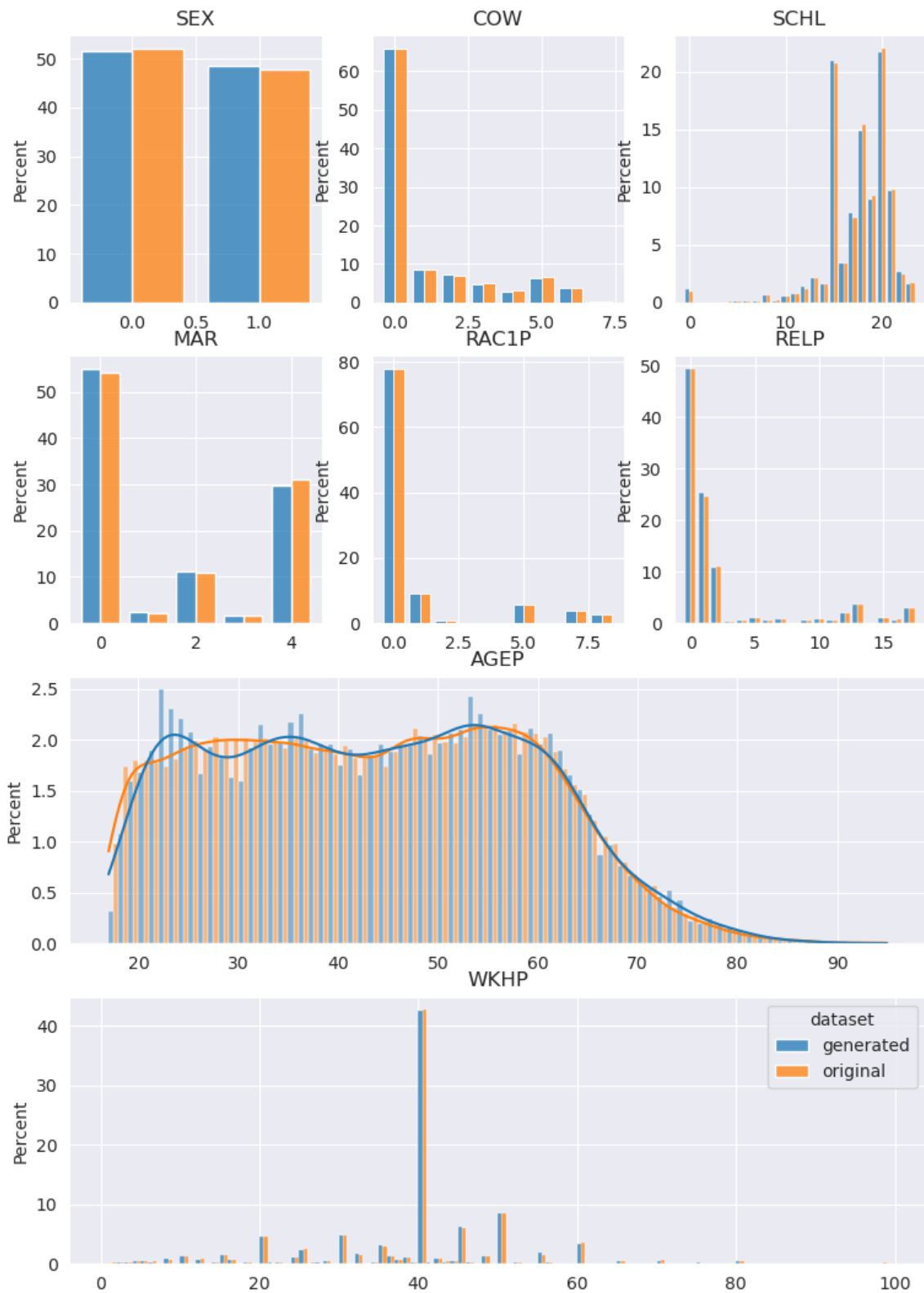


Figure 6: **MiniACSIIncome Bayesian Network – Marginal Distributions.** The ‘generated’ data is sampled from the Bayesian Network, while the ‘original’ data is the MiniACSIIncome-8 dataset.

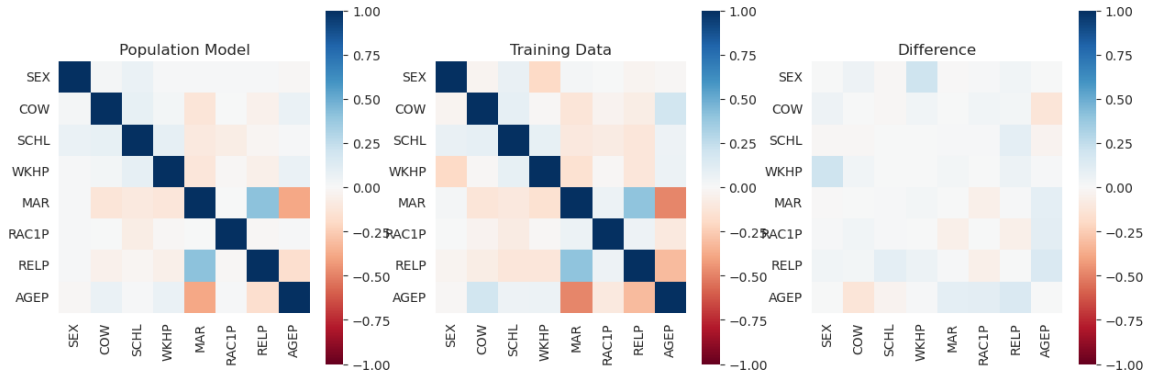


Figure 7: **MiniACSIncome Bayesian Network – Correlation Matrix.** ‘Population Model’ denotes the fitted Bayesian Network, while ‘Training Data’ stands for the full MiniACSIncome-8 dataset.

datasets. All networks are trained using: the Adam optimiser [35], cross entropy as loss function, no  $L_2$  regularisation (weight decay),  $\beta_1 = 0.9$ ,  $\beta_2 = 0.999$ ,  $\varepsilon = 10^{-8}$  as suggested by Kingma and Ba [35], and a learning rate decay by 0.1 after 2000 and 4000 iterations. The learning rate and the number of training epochs are contained in Table 10. For each network, we perform five random restarts and select the network with the lowest cross entropy on the validation data.

Table 11 contains the accuracy, precision, and recall for the overall test set, the persons with female sex in the test set, and the persons with male sex in the test set. Additionally, the table contains whether a network satisfies the demographic parity fairness notion according to PV.

We used Optuna [2] for an initial exploration of the hyperparameter space but did not apply automatic hyperparameter optimisation to obtain the final training hyperparameters.

<b>Dataset</b>	<b>Architecture</b>	<b>Learning Rate</b>	<b># Epochs</b>
MiniACSIIncome-1	1×10	0.0001	1
MiniACSIIncome-2	1×10	0.001	2
MiniACSIIncome-3	1×10	0.001	3
MiniACSIIncome-4	1×10	0.001	4
MiniACSIIncome-5	1×10	0.001	5
MiniACSIIncome-6	1×10	0.001	3
MiniACSIIncome-7	1×10	0.001	3
MiniACSIIncome-8	1×10	0.001	3
MiniACSIIncome-4	1×1000	0.001	2
MiniACSIIncome-4	1×2000	0.001	2
MiniACSIIncome-4	1×3000	0.001	2
MiniACSIIncome-4	1×4000	0.001	2
MiniACSIIncome-4	1×5000	0.001	2
MiniACSIIncome-4	1×6000	0.001	2
MiniACSIIncome-4	1×7000	0.001	2
MiniACSIIncome-4	1×8000	0.001	2
MiniACSIIncome-4	1×9000	0.001	2
MiniACSIIncome-4	1×10 000	0.001	2
MiniACSIIncome-4	2×10	0.001	2
MiniACSIIncome-4	3×10	0.001	2
MiniACSIIncome-4	4×10	0.001	2
MiniACSIIncome-4	5×10	0.001	2
MiniACSIIncome-4	6×10	0.001	2
MiniACSIIncome-4	7×10	0.001	2
MiniACSIIncome-4	8×10	0.001	2
MiniACSIIncome-4	9×10	0.001	2
MiniACSIIncome-4	10×10	0.001	2

Table 10: **MiniACSIIncome Training Hyperparameters.**

Dataset	Net	Overall			Female			Male			Fair?
		A	P	R	A	P	R	A	P	R	
mACSI-1	1×10	57%	44%	63%	72%	–	0%	44%	44%	100%	×
mACSI-2	1×10	65%	55%	14%	71%	–	0%	58%	55%	23%	×
mACSI-3	1×10	73%	67%	48%	76%	65%	35%	69%	68%	55%	×
mACSI-4	1×10	75%	68%	60%	78%	66%	48%	72%	69%	66%	×
mACSI-5	1×10	76%	69%	63%	79%	65%	53%	74%	71%	69%	×
mACSI-6	1×10	77%	69%	63%	79%	65%	55%	74%	72%	68%	×
mACSI-7	1×10	77%	71%	64%	79%	67%	50%	76%	72%	72%	×
mACSI-8	1×10	78%	70%	68%	80%	67%	56%	76%	71%	75%	?
mACSI-4	1×1000	75%	71%	54%	79%	70%	44%	72%	71%	61%	×
mACSI-4	1×2000	75%	65%	67%	78%	61%	60%	72%	67%	71%	✓
mACSI-4	1×3000	74%	63%	71%	77%	58%	67%	72%	66%	73%	✓
mACSI-4	1×4000	75%	71%	55%	79%	69%	44%	72%	71%	61%	×
mACSI-4	1×5000	75%	69%	58%	78%	71%	39%	73%	68%	69%	×
mACSI-4	1×6000	75%	69%	59%	79%	69%	44%	72%	68%	67%	×
mACSI-4	1×7000	75%	66%	64%	78%	62%	55%	72%	68%	68%	×
mACSI-4	1×8000	75%	66%	64%	78%	63%	55%	72%	68%	69%	×
mACSI-4	1×9000	75%	70%	53%	78%	66%	47%	71%	72%	56%	×
mACSI-4	1×10 000	75%	67%	63%	79%	69%	45%	72%	66%	73%	×
mACSI-4	2×10	75%	67%	59%	78%	65%	48%	72%	69%	65%	×
mACSI-4	3×10	75%	68%	58%	79%	67%	47%	72%	69%	65%	×
mACSI-4	4×10	75%	68%	58%	78%	66%	46%	72%	69%	66%	×
mACSI-4	5×10	75%	68%	59%	78%	67%	47%	72%	69%	66%	×
mACSI-4	6×10	75%	67%	61%	78%	67%	46%	72%	67%	70%	×
mACSI-4	7×10	75%	65%	66%	78%	63%	52%	72%	65%	74%	×
mACSI-4	7×10	75%	67%	59%	78%	65%	46%	72%	68%	67%	×
mACSI-4	9×10	75%	67%	59%	78%	65%	47%	72%	68%	67%	×
mACSI-4	19×10	75%	67%	61%	78%	64%	49%	72%	68%	68%	×

Table 11: **MiniACSIIncome Neural Networks.** The abbreviation ‘mACSI-*i*’ stands for MiniACSIIncome-*i*. We report the accuracy (A), precision (P), and recall (R) of each trained network (Net) for the whole test dataset (Overall), the persons with ‘SEX=2’ in the test set (Female), and the persons with ‘SEX=1’ in the test set (Male). Additionally, we report whether the network satisfies the demographic parity fairness notion according to PV (Fair?).

## D Heuristics for ProbBounds

This section contains motivation and additional implementation details for our BaBSB Split heuristic and compares the different branch and split selection heuristics that we introduce in Section 4.2.

### D.1 BaBSB

Our BaBSB split selection heuristic is a variation of the BaBSB heuristic for non-probabilistic neural network verification of Bunel et al. [15]. One difference is that Bunel et al. [15] use the method of Wong and Kolter [62] for estimating the improvement in bounds, while we use interval arithmetic. Another difference is that while Bunel et al. [15] are mainly interested in lower bounds, we are equally interested in lower and upper bounds. Therefore, we select the dimension  $d$  that yields the largest lower bound or smallest upper bound in any of the new branches, while Bunel et al. [15] select the dimension  $d$  with the largest lower bound among the smaller lower bound for the two branches originating from splitting  $d$ . We found this variant to be the most successful for our application. Bunel et al. [15] discuss further variants.

**Implementation.** We round all bounds to four decimal places to mitigate floating point issues. If several dimensions yield equal improvements in bounds, we randomly select one of these dimensions. Without this random tie-breaking, we might split a single dimension repeatedly if the interval arithmetic bounds are very loose. We use a separate pseudo-random number generator with a fixed seed for this tie-breaking so that BaBSB remains entirely deterministic.

### D.2 Experiments

We compare the branch selection heuristics SelectProb and SelectProbLogBounds when running PV on a selection of the benchmarks from Section 6. In both cases, we use CROWN [67] to compute bounds on  $g_{\text{Sat}}(\mathbf{x}, \text{net}(\mathbf{x}))$  and use our BaBSB split selection heuristic. We do not provide a detailed comparison of LongestEdge and BaBSB since LongestEdge does not allow PV to solve even the least demanding FairSquare benchmarks within the time budget of 15 minutes.

Unlike the experiments in Section 6 and Appendix C, we use recent hardware for comparing the different ProbabilityBounds heuristics. Concretely, we use a compute server running Ubuntu 22.04 with an AMD Ryzen Threadripper 3960X CPU with 24 cores and 252 GB of memory (HW2).

We compare SelectProb and SelectProbLogBounds on the FairSquare benchmarks, the ACAS Xu robustness benchmark, and MiniACSIncome-1 to MiniACSIncome-6. We note that this set contains many less demanding instances. Figure 8 visualises the results. SelectProbLogBounds has a slight advantage over SelectProb, meaning that PV can solve a few more instances and can solve a few other instances faster when using SelectProbLogBounds compared to SelectProb.

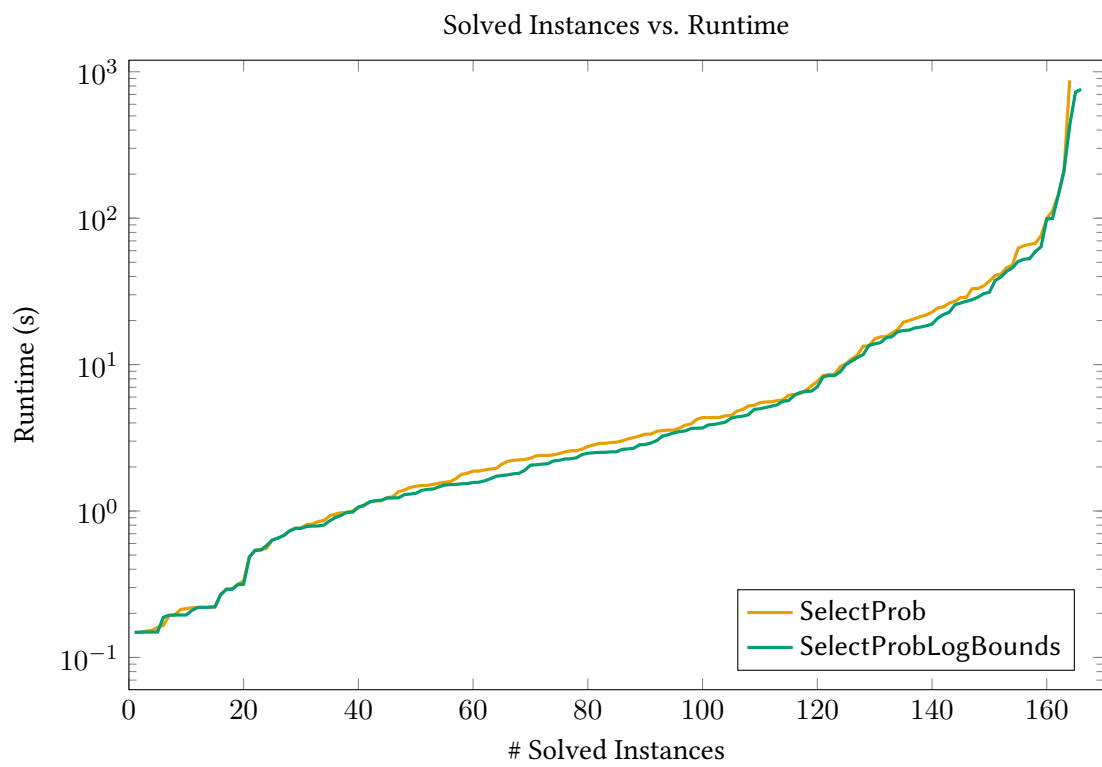


Figure 8: **SelectProb vs. SelectProbLogBounds**. Lower is better.